R. & M. No. 3246

MINISTRY OF AVIATION

AERONAUTICAL RESEARCH COUNCIL
REPORTS AND MEMORANDA

An Experimental Investigation of Heat Transfer from the Inside Surface of a Hot Smooth Tube to Air, Helium and Carbon Dioxide

By J. F. Barnes

LONDON: HER MAJESTY'S STATIONERY OFFICE
1961
FIFTEEN SHILLINGS NET

An Experimental Investigation of Heat Transfer from the Inside Surface of a Hot Smooth Tube to Air, Helium and Carbon Dioxide

By J. F. Barnes

Communicated by the Deputy Controller Aircraft (Research and Development), Ministry of Aviation

*Reports and Memoranda No. 3246**
March, 1960

Summary. This Report gives experimental values of Nusselt number as a function of Reynolds number and surface/gas temperature ratio for three gases, air, helium and carbon dioxide, and shows the effects of radial variations of fluid properties with temperature. The conditions under which the experiments were performed were fully developed velocity and temperature profiles and subsonic turbulent flow. These conditions are typical of those encountered in the cooling passages of a nuclear reactor or a turbine blade.

The experimental results are presented in a form suitable for use in design work and are compared with existing experimental and theoretical data.

1.0. *Introduction.* Accurate heat transfer data are required in many aspects of present day design work. Two particular examples, closely associated with the experimental work described in this Report, are the cooling by forced convection of turbine blades[1] with air pumped through spanwise passages formed in the blade, and the removal of heat by forced convection from gas cooled nuclear reactors[2]. In both of these examples it is necessary to be able to predict accurately the surface temperature distribution in the cooling passages corresponding to any given set of coolant gas conditions. For the turbine blade, the strength properties of the blade material will be critically dependent on temperature. This may be also true of the materials in a nuclear reactor, but in addition the reactivity of the fissile material tends to fall as its temperature rises, and consequently the fissile material has to be reprocessed more frequently, with an attendant increase in the cost of power production. Hence the need for accurate heat transfer data, particularly when the surface temperature is very much greater than the average or bulk temperature of the gas flowing through the cooling passages. Under these conditions there is an appreciable radial variation of gas temperature from the centre of the passages to the surface and the effects on the rate of heat transfer of variations in temperature-dependent gas properties cannot be neglected. Previous work[3, 4, 5, 6, 7] has shown both theoretically and experimentally for the turbulent flow of air in smooth pipes of circular cross section that as the ratio of the surface absolute temperature to the air bulk absolute temperature increases, the Nusselt number† falls, provided that the Reynolds number is kept constant and that both these last parameters are evaluated with air properties taken at the bulk temperature. There

* Previously issued as N.G.T.E. Report No. R.241—A.R.C. 21,991.

† For definitions *see* Appendix I.

is however, little published information[4] on the behaviour of the other gases such as helium and carbon dioxide which are more suitable than air for the nuclear reactor application.

The object of the work reported here was to measure the effects of temperature ratio on Nusselt number for helium and carbon dioxide flowing in smooth pipes of circular cross section in the bulk Reynolds number range from 4,000 to 60,000. This range of Reynolds numbers appears to cover the region of greatest interest in reactor design work. In addition measurements were made during the preliminary testing and development of the apparatus using air and (for a few points) argon as the working fluids. The technique used to measure Nusselt numbers differed from that used in previous reported work[3] and the measured effects of surface/gas temperature ratio for air are not exactly the same. The reasons for this difference are given later and it is sufficient to state here that in the present work all the heat transfer measurements were confined to a region where both the radial velocity and temperature profiles were fully developed and both entrance effects and end effects were eliminated. Such conditions are likely to be representative of actual applications, particularly so for the cooling of nuclear reactors where the cooling passages will usually have length/hydraulic diameter ratios of the order of 100 or more.

For all three gases the range of surface/gas temperature ratio at which measurements were made lies between 1 and 2·2 and most of the measurements were made with the gas bulk temperature in the range 300 deg K to 400 deg K. Some additional experiments were conducted with air and helium preheated to 600 deg K. The highest Mach numbers during testing were obtained with helium as working substance. Efforts were made to avoid average Mach numbers greater than 0·3 with helium by raising the pressure and density levels in the apparatus, so that the flow conditions would be truly representative of the 'incompressible' flow generally associated with reactor cooling.

In addition to a description and explanation of the experimental results, a detailed description of certain parts of the apparatus is included because they embody certain novel features which may be of interest to other workers in this field.

2.0. *Description of Apparatus.* Previous work[7] demonstrated the feasibility of the technique for measuring Nusselt numbers in the region of the test section where radial velocity and temperature profiles were fully developed. These experiments were performed on a very simple rig using compressed air from the laboratory supply and discharging the heated air to atmosphere. It was obvious, however, that such a technique would lead to prohibitively high operating costs if used with helium as the working substance, and therefore that a closed cycle apparatus would have to be constructed, with very careful attention paid to the problem of leakage, so that a small quantity of helium could be circulated repeatedly and only a small make-up supply would be needed to cope with leakage during operation. Full details of this closed cycle apparatus are given in Appendix II, and a flow diagram and electrical circuit are included in Figures 1 and 2.

Also in Appendix II there is a detailed description of the three electrically heated test sections used for the experiments, and some of the details of their construction are shown on Figure 3. All three tubes were made of stainless steel and had the following dimensions:

TABLE 1

Test section	No.	1	2	3
Tube inside diameter	in.	0·247	0·553	0·246
Heated length	in.	12	24	12
Starting length	in.	14	24	9

Most of the testing at gas average bulk temperatures between 300 deg K and 400 deg K was performed with the first test section. The second was used to obtain data at low Reynolds numbers (up to 10,000) and the third was used with air or helium preheated to about 600 deg K.

3.0. *Experimental Procedure.* The first test of any series using a given test section was conducted with no gas flowing through the system at a series of low electrical input powers. By this means the heat losses from the tube to the lagging could be obtained for various tube wall temperatures. This heat loss information was used in subsequent tests to deduce the net electrical power given to the gas. For this purpose allowances had to be made for conduction losses axially along the pipe and radially outwards to the lagging.

During the actual tests with gas flowing through the test section, the mass flow was kept as constant and as steady as possible, and the electrical power was raised progressively by finite amounts. The pressure in the test section was kept high enough to maintain the average Mach numbers at less than 0·3 for helium: for other gases the Mach numbers never exceeded 0·2. When the tube wall temperatures and the gas temperatures became steady for any set of conditions, the current and voltage drops along the test section were read, together with the orifice readings and the gas and wall temperatures. As explained in Appendix II, the heater power at the exit end of the test section was adjusted so that the thermocouples embedded in the piece of the test section were recording temperatures as nearly as possible equal to that recorded by the gas exit thermocouple. Generally one set of readings took about five minutes and the time required for the rig to settle down varied considerably from times as short as five minutes when running with helium at high mass flows to one hour when initially warming up the third (high temperature) test section and its mixing chambers. During the experiments the pump unit and its controls required little attention apart from small changes in the settings of the by-pass and make-up valves.

4.0. *Reduction of Data.* From the readings taken it was possible to compute the enthalpy received by the gas, using the measured mass flow and temperature rise and the specific heat of the gas at constant pressure, evaluated at the arithmetic mean of the inlet and outlet temperatures. Also it was possible to allow for heat losses and to obtain the net electrical power given to the gas, and compare this with the measured enthalpy rise. For tests without preheating of the gas these heat balances usually agreed to within 3 per cent for helium and the corresponding maximum discrepancies for air and carbon dioxide were 5 and 6 per cent respectively at Reynolds numbers above 8,000. Below this Reynolds number, the heat balances became progressively worse, and for the few tests performed with air and helium at around 1,000, the error was as great as 15 per cent in isolated cases. It is believed that the errors lay chiefly in the measurement of the gas outlet temperature, so that the electrical measurements were regarded as more reliable. The reason for this belief arose from experience in the use of a guard heater wound on a brass cylinder around, but separated from, the thermocouple used to measure the gas exit bulk total temperature. It was intended that the power supply to this heater would be adjusted to minimise heat losses by conduction from the gas mixer to the rest of the mixing chamber body. This mixer was connected to the cylinder of the guard heater by a thin brass disc containing two thermocouples at different radii (*see* Fig. 3). The adjustment of the power supply was to be regarded as satisfactory when the disc temperatures were themselves equal and agreed as closely as possible with the reading of the gas exit thermocouple. In tests at the higher Reynolds numbers it was found that the reading of the gas exit thermocouple was relatively insensitive to changes in the disc temperatures arising from

changes in the power supply to the guard heater. However, as the Reynolds number was reduced, the readings of the gas exit thermocouple became more sensitive to changes in the disc temperatures. It was then difficult to maintain a steady reading of the gas exit thermocouple because of the slow response of the disc temperatures to changes in power supply. With preheated gas, considerable difficulty was experienced in obtaining steady conditions and for many of the results heat balances differed by 10 per cent, and in some instances, even more.

In addition to obtaining a heat balance, the measured values of the electrical energy given to the gas along the four equal sections of the heated length were used to calculate the distribution of gas bulk total temperature along the tube (*see* Fig. 2). This distribution was not exactly linear, so that the average gas bulk temperature over the middle 6 in. of the tube was not exactly equal to the arithmetic mean of the measured temperatures. The former average gas bulk temperature deduced from the calculated distribution was used to find the average heat transfer coefficient for the middle 6 in., and the gas properties were based on this temperature in the calculation of Nusselt, Reynolds and Prandtl numbers.

The average wall temperature for the middle 6 in. was obtained by plotting the wall temperature distribution as in Fig. 2 and finding the area underneath this part of the curve. From this, the average surface temperature in the middle 6 in. was calculated using the formula

$$\overline{T}_w - \overline{T}_s = \frac{H}{2\pi LK}\left[\frac{\log_e (r_0/r_i)}{[1-(r_i/r_0)^2]} - \frac{1}{2}\right]. \tag{1}$$

The Notation is given in Appendix I. The heat transfer coefficient for this section was computed using the difference between the average surface temperature and the average gas bulk total temperature, *viz.*,

$$h = \frac{H}{2\pi r_i L(\overline{T}_s - \overline{T}_b)}. \tag{2}$$

Then the Nusselt number was obtained from

$$Nu_b = \frac{hD}{\lambda_b} \tag{3}$$

and the corresponding Reynolds number from

$$Re_b = \frac{4Q}{\pi D\mu_b}. \tag{4}$$

The gas properties used in the evaluation of these parameters are shown in Fig. 4, for air, helium and carbon dioxide. They are based on Ref. 8. (The tests with argon were done primarily to prove the rig before using the helium supplies and although the few results obtained have been included, the argon properties have not been shown. They were obtained from Ref. 10.) A short discussion of gas properties is included in Appendix I.

During any given test at constant mass flow, the Reynolds number tended to fall as T_b (and μ_b) increased with increasing heat input. In order to be able to plot the Nusselt numbers against surface/gas temperature ratio T_s/T_b at any given Reynolds number (Figs. 5, 6 and 7) the Nusselt numbers were corrected to a constant value of Reynolds number for any given test by assuming

$$Nu_b \propto Re_b^{0\cdot8} \quad (Re_b > 9{,}000)$$

or (5)

$$Nu_b \propto Re_b^{0\cdot9} \quad (4{,}000 < Re_b < 9{,}000).$$

The Reynolds number variation throughout a given test was not large, so that the correction amounted to only 2 or 3 per cent. Some results were obtained also for Re_b values less than 4,000. These were not plotted but were used in the construction of Figs. 9 and 10.

The reason for computing the average Nusselt number over only the middle 6 in. of the test section is that 'end effects' are eliminated. When the gas bulk temperature and the surface temperature both increase axially in the same manner, *e.g.*, linearly or nearly so in these experiments, the temperature profile is fully established. The velocity profile has also been allowed to develop sufficiently to be regarded as fully established so that the conditions under which the Nusselt number has been measured can be stated emphatically to be

(i) fully developed velocity profile,

(ii) fully developed temperature profile, and

(iii) essentially low subsonic turbulent flow conditions ($\overline{M} < 0{\cdot}3$).

This means that the measured temperature ratio effects produced by radial variation of fluid properties with temperature will be the same as those occurring in a reactor cooling passage of large length/hydraulic diameter ratio (> 100) where end effects are small.

It has been demonstrated that if the wall temperature is rising more quickly than the gas bulk temperature along the pipe, then the rate of heat transfer is greater than for equal rates of axial temperature rise and *vice versa*[9]. It might be thought that effects due to large positive and negative axial wall temperature gradients at the inlet and outlet ends of the test section respectively may tend to be substantially equal and opposite, hence cancelling each other out: this may be so but it is obviously much better to eliminate these effects completely if at all possible. Other reasons why these end effects should be eliminated will be given later (Section 6.2).

The reasons for basing the fluid properties on the gas bulk *total* temperature and for expressing the temperature ratio effects using this temperature are that in design work total temperatures are much more likely to be known than static values, which depend on the mass flow in any given passage and on the passage cross-section area, both of which may be unknowns[2].

5.0. *Test Results.* In Figs. 5 to 12 the parameter $Nu_b/Pr_b^{0{\cdot}4}$ is plotted as a function of Re_b and T_s/T_b. This method of plotting the results facilitates comparison with the well established relationship used when there is negligible variation of gas properties with temperature in the radial plane. This relationship is often expressed as

$$Nu = (\text{constant})\ Re^{0{\cdot}8}\ Pr^{0{\cdot}4} \tag{6}$$

$$Re > 8{,}000\,.$$

The value of the constant used in this equation depends on the pipe geometry (length/diameter ratio) and also on the distribution of wall temperature. For the length/diameter ratios used and the wall temperature distributions obtained in this work, the constant can be assumed equal to $0{\cdot}023$. The experimentally observed values of the parameter $Nu_b/Re_b^{0{\cdot}8}\ Pr_b^{0{\cdot}4}$ should approach $0{\cdot}023$ as T_s/T_b approaches unity.

As described in Section 4.0, the experimentally obtained Nusselt numbers were corrected for slight variations in Reynolds number so that sets of points could be plotted for various constant values of Reynolds number, in order to find the effect of T_s/T_b. This is done in Fig. 5 for air, at

Reynolds numbers exceeding 4,000, with bulk air temperatures in the range 300 deg K to 400 deg K. The few test points obtained at lower Reynolds numbers were not very accurate and it was felt that no useful purpose would be served in trying to extract any data from them on the effects of temperature ratio. The data for $Re_b \geqslant 9{,}000$ in Fig. 5 were obtained from Test Section No. 1. For $Re_b \leqslant 9{,}000$, Test Section No. 2 was used and the two sets of points for $Re_b = 9{,}000$ provide a useful confirmation that the results from the two sections can be considered together. When plotted on logarithmic paper as in Fig. 5 the experimental points indicate that for design purposes at any given Reynolds number the effect of surface/gas temperature ratio can be expressed conveniently as

$$Nu_b = C\, Re_b^{0\cdot8}\, Pr_b^{0\cdot4} \left(\frac{T_s}{T_b}\right)^m \tag{6a}$$

where m is the slope of the line drawn through test points for that Reynolds number. Also points are shown at $T_s/T_b = 1$ which are calculated from Equation (6) and it is seen that for $Re_b \geqslant 10{,}000$, Equation (6) does indeed apply to the experimental data extrapolated to $T_s/T_b = 1$. At temperature ratios less than $1\cdot1$, the actual difference between surface and gas temperature which is used to calculate the Nusselt number becomes small compared with the temperature rise experienced by the gas and any errors in the bulk temperature values cause scatter, especially at the lower Reynolds numbers.

In Fig. 6 the helium results for $Re_b \geqslant 4{,}000$ are presented, again for gas bulk temperatures between 300 deg K and 400 deg K. All the results for $Re_b \geqslant 6{,}000$ were obtained using Test Section No. 1, and those below 6,000 were obtained with Test Section No. 2. The two sets of points at $Re_b = 6{,}000$ again confirm that experimental results from the two test sections can be considered together. The results are generally similar to those obtained for air. Two differences are that the effect of temperature ratio does not appear to be as great for helium as it is for air and Equation (6) would appear to apply at Reynolds numbers as low as 6,000 when T_s/T_b approaches unity.

The results obtained for carbon dioxide are shown in Fig. 7. All except the points for $Re_b = 8{,}000$ were obtained with Test Section No. 1. The results show a temperature ratio effect similar to the other gases and also that Equation (6) applies when T_s/T_b tends to unity.

Similarly in Fig. 8, some heat transfer results for argon are shown. They were obtained during the final development of the rig, prior to testing with helium.

The straight lines through the test points in Figs. 5, 6 and 7 were drawn in order to cross plot the test results in Figs. 9, 10 and 11 where $Nu_b/Pr_b^{0\cdot4}$ is plotted against Re_b for values of T_s/T_b equal to $1\cdot2$, $1\cdot4$, $1\cdot6$, $1\cdot8$ and $2\cdot0$. In addition, a straight line corresponding to Equation (6) is shown in each figure. For clarity, test points have not been recorded in any of these three figures which are regarded as being the most convenient way of presenting the heat transfer data for use in design work.

In Fig. 12, the test results obtained with Test Section No. 3 are recorded. Considerable trouble was experienced in obtaining steady conditions and satisfactory heat balances during these tests; hence the scatter. All that can be concluded from these results is that if they are expressed in the form of Equation (6a), then the values of the constants C and m deduced from the tests without preheated gas give Nusselt numbers which are in moderate agreement with the observed results. For all four gases, the values of C can be assumed to be $0\cdot023$, plus or minus 3 per cent. The average values of m over the Reynolds number range considered are given in the following table.

TABLE 2

Gas	Average slope of lines shown on FIGS. 5, 6, 7 and 8 'm'.
Air ..	−0·40
Helium ..	−0·185
CO_2 ..	−0·27
Argon ..	−0·43

6.0. *Discussion.* 6.1. *Observed Effects of Surface/Gas Temperature Ratio and Comparison with Theory.* When the bulk Reynolds number is kept constant it is seen that for all three gases, the Nusselt number (Nu_b) falls as the surface/gas temperature ratio (T_s/T_b) is increased. It is believed that this effect of temperature ratio can be explained by considering the changes which occur in the fully developed temperature profile at any chosen axial position in a tube when the mass flow and bulk gas total temperature (and hence Re_b) are kept constant and the surface temperature is allowed to rise. The tubes used for the experimental work are too small to permit accurate temperature traversing so recourse must be made to the theoretical work of Refs. 5 and 6, which are described in Appendix III. This theoretical approach is to obtain velocity and temperature profiles in non-dimensional forms by simultaneous integration of the equations for radial transfer of heat and momentum. In order to perform these integrations it is assumed that the transfer of heat and momentum in the turbulent region of the flow occurs in the same manner. Also data must be used which are derived from experimental measurements of velocity profiles at a temperature ratio of unity. The assumptions which are made for the variation of gas properties with temperature correspond most nearly to helium.

The results of the integrations are that profiles of non-dimensional velocity, u^+, and temperature, t^+, can be plotted as functions of y^+, a non-dimensional distance from the walls of a circular pipe, for various values of a heat loading parameter β, which is positive for heat addition to the gas and *vice versa.* The definitions of u^+, t^+, y^+ and β are given in Appendix III.

In this Appendix the method is described whereby unique values of Nu_b, T_s/T_b, and Re_b are deduced from integrations of the non-dimensional velocity and temperature profiles with previously chosen values of β and r^+, corresponding to the tube radius in non-dimensional form. Some trial and error is involved in the choice of β and r^+ if particular values of T_s/T_b and Re_b are specified. If Re_b is fixed, the required values of r^+ decrease as T_s/T_b is increased, so that any fixed value of y^+ corresponds to an increasing distance from the pipe wall. Since it can be deduced[5, 6] that u^+ and t^+ vary linearly with y^+ near the wall ($0 \leqslant y^+ \leqslant 5$), this implies that the slopes of the velocity and relative temperature profiles become less steep relative to the pipe radius as T_s/T_b rises and Re_b is kept constant. This is illustrated in Fig. 13 where relative temperature profiles (in terms of $(T_s - T)/(T_s - T_b)$) are plotted for a bulk Reynolds number of 11,800 and values of T_s/T_b equal to 1·0 and 1·58 respectively. Fig. 14 shows exactly similar data for a bulk Reynolds number of 221,000 and temperature ratios of 1·0 and 1·59 respectively. From both figures it will be seen that there is little change in the overall profile as T_s/T_b is altered, but the lower diagram on each figure

indicates that there is an appreciable reduction in the relative temperature gradient near the wall as T_s/T_b rises. Since by definition all the heat transfer in the laminar sub-layer near the wall must be by conduction, it is possible to express the heat flux at the pipe surface in terms of the thermal conductivity and the temperature gradient in the laminar sub-layer, and therefore to deduce expressions for the heat transfer coefficient and Nusselt number. This is done in Appendix III and shows that when the surface/gas temperature ratio is increased, and the gas bulk Reynolds number is kept constant, the Nusselt number falls because of the reduction in the relative temperature gradient within the laminar sub-layer. As the pipe surface temperature rises, the thermal conductivity in the laminar sub-layer also rises, but not at a rate which is great enough to counteract the effect of the reduced relative temperature gradient.

The results of some of these calculations are plotted in Fig. 15. Comparison of Figs. 9 and 15 shows that the actual values of $Nu_b/(Pr_b)^{0\cdot4}$ do not agree closely, except at $Re_b = 15{,}000$. At high Reynolds numbers the calculated values of $Nu_b/(Pr_b)^{0\cdot4}$ are too small and the method predicts temperature ratio effects which are apparently too great. No definite reason can be given to explain why the calculations should show a temperature ratio effect which increases with Reynolds number, when the opposite is observed experimentally for three of the gases tested. It would appear that this particular theoretical approach is only of value in giving a reasonable qualitative explanation of the fall in Nu_b as T_s/T_b rises and Re_b is kept constant.

It must be emphasized that all the theoretical work in Refs. 5 and 6 is based on measurements made for velocity profiles at a temperature ratio of unity and that heat and momentum transfer in the turbulent region of the flow are assumed to occur in exactly the same manner. There is little information available at present to permit a different approach: all one can do is to alter certain basic assumptions and try more realistic expressions for variations of gas properties with temperature and for the variation of heat flux across the pipe, in the hope that better agreement will result.

Better agreement has been obtained between theory and experiment in Ref. 13, where more realistic transverse distributions of heat flux and shear stress have been assumed. Different variations of fluid properties with temperature were incorporated to allow comparisons for helium and carbon dioxide as well as air. However, it was still necessary to employ data deduced almost exclusively from isothermal velocity and temperature profiles, and it is emphasised[13] that more information is desirable concerning the transfer of heat and momentum, under non-isothermal conditions over a wide range of Reynolds number. It is believed therefore that satisfactory agreement may not be obtained until detailed measurements are available for velocity and temperature profiles, especially in the vicinity of the tube surface, with surface/gas temperature ratios appreciably different from unity. It is also concluded in Ref. 13 that the radial variations of density and specific heat in the terms describing the turbulent transfer of heat and momentum are the main cause of the changes in the shapes of the velocity and temperature profiles, as the surface/gas temperature ratio is increased at constant bulk Reynolds number. Over most of the flow the effects of these turbulent transport terms are shown to dominate completely any influence of viscosity and thermal conductivity on the shapes of the velocity and temperature profiles. (This could also be deduced from an inspection of Equations (5) and (6) of Appendix III, using the variations of shear stress, heat flux and diffusivities specified in Ref. 6.)

Fig. 16 shows the theoretical temperature, density and viscosity profiles for helium plotted as T/T_b, ρ/ρ_b and μ/μ_b at Reynolds numbers of 11,800 and 221,000 and at a value of T_s/T_b approximately equal to $1\cdot6$. It will be seen that the deviation of properties from the bulk values is smaller at the

higher Reynolds number, suggesting in a purely qualitative manner that when gas properties are evaluated at the bulk temperature, the effect of temperature ratio should become smaller as the Reynolds number increases.

6.2. *Comparison of Present Experimental Work with Other Published Experimental Data.* As previously stated in Section 4.0, the portion of the tube in which heat transfer coefficients and Nusselt numbers were measured was where the temperature and velocity profiles could be assumed to be fully developed, and the effects of rapid axial changes of surface temperature on the heat transfer rate were avoided.

Referring to the temperature distribution drawn in Fig. 2, which is for a relatively modest surface/gas temperature ratio, theoretical calculations based on Ref. 9 show that in the first quarter of the test section the *average* heat transfer coefficient is approximately 4 per cent greater than the average value for the middle 6 in. of the section, where the actual measurements were made. Similarly, over the final quarter, the average coefficient is (theoretically) 6 per cent lower than the measured average value, and what is more important, the theory predicts that heat is actually transferred from the gas to the wall in the final region where the wall temperature is falling steeply. The reason for this last effect is that, although the bulk gas temperature may be less than the wall temperature, the latter is falling sufficiently steeply for only the outer gas layers to be affected, with the result that the temperature profile near the wall suffers a reversal. Obviously the gas temperature adjacent to the wall must be equal to the wall temperature itself to maintain finite rates of heat transfer. (*See* Fig. 17 and Ref. 9.) Much of the existing experimental data for heat transfer from the inside walls of a tube to air under conditions of turbulent flow is based on measurements made over the whole of the heated section. In view of the very steep axial temperature gradients which can occur at each end of the heated section (*see*, for example, Ref. 3) it is not unreasonable to suspect that heat can be lost from the air to the tube walls in the section immediately upstream of the thermocouples measuring the air exit temperature. It must be remembered that even with a satisfactory heat balance between the electrical energy supplied to, and the heat received by the air, such an effect could escape unnoticed unless measurements are made of the distribution of energy supplied to the air over various sections of the tube.

The steep axial wall temperature gradients therefore cause the gas bulk total temperature to rise in a non-linear manner from the inlet to the outlet of the heated section, so that the arithmetic mean of the measured inlet and outlet gas temperatures does not coincide with the deduced gas bulk total temperature at the mid point of the tube. As the surface/gas temperature ratio is increased, the difference between the arithmetic mean of the measured temperatures and the deduced bulk temperature at the mid point is also increased. Heat transfer data deduced from measurements over the whole of the heated section, using gas properties and heat transfer coefficients based on the arithmetic mean temperature, cannot therefore be expected to agree with data based on measurements made over the mid-section of the tube, as in the present investigation, especially at large surface/gas temperature ratios.

The difference between the measured effects of surface/air temperature ratio in Ref. 3 and those in this Report is appreciable. In fact the data given in Ref. 3 suggest an effect of the form $(T_s/T_b)^{-0\cdot55}$, whereas the present work for air results in an average index of $-0\cdot4$ in Equation (6a) rather than $-0\cdot55$, and it is believed that the explanation for this difference lies in the phenomena described in the preceding paragraphs of this section.

The boundary conditions of the experiments described in the present Report have been clearly defined (Section 4.0) and are held to be much more representative of coolant conditions in a nuclear reactor where the passages are likely to be of large length/diameter ratio (> 100) and end effects are of little importance. A second minor point is that for theoretical calculations it is very much easier to compare theory with experiment when the velocity and temperature profiles are fully developed.

Very limited data are available for heat transfer from a hot surface to gases other than air, especially helium. Ref. 4 contains some information on the heating and cooling of carbon dioxide and on the cooling of helium. The data for the heating of carbon dioxide is unfortunately confined to a Reynolds number range above 80,000, where the general conclusion is that the surface/gas temperature ratio effect is similar to that measured in this work and that theory (similar to Ref. 6) underestimates the Nusselt number values.

In Ref. 12, experimental values of Nusselt number, based on local heat transfer coefficients from the surface of a hot tube to helium, are presented for surface/gas temperature ratios from $1 \cdot 8$ to $3 \cdot 9$. All the helium properties are evaluated either at the surface temperature or at a film temperature which is the arithmetic mean of the surface and the gas bulk total temperatures, but it is possible to convert the results to values based on bulk temperature. When this is done, the one point for $T_s/T_b = 1 \cdot 8$ is $Nu_b/(Pr_b)^{0 \cdot 4} = 57 \cdot 6$ at $Re_b = 22{,}300$, and this agrees very well with Fig. 10. For $T_s/T_b = 1 \cdot 9$, there are three points, all of which lie within the limits of experimental error when compared with extrapolated values from Fig. 10. At higher values of T_s/T_b, the experimental results usually follow the expected trend, but without exception they fall well below the values predicted by Equation (6a). There are also some anomalies, which cannot be explained away satisfactorily as rounding off errors in the presentation and subsequent conversion of the data: some points for $T_s/T_b = 2 \cdot 8$ lie above those for smaller values of surface/gas temperature ratio.

At higher levels of temperature, the results of different investigators cannot be compared with each other unless a critical comparison of the gas properties used to evaluate Nusselt, Reynolds and Prandtl numbers is made at the same time. It is well known that, of the gas properties needed in this field, the thermal conductivity is the most difficult to measure accurately, and quoted values may vary considerably, especially at temperatures above 500 deg K, where in some instances it has been necessary to rely on extrapolations. In Ref. 3, where extrapolated values of thermal conductivity were used, the measured Nusselt numbers fell as the gas temperature rose, with Reynolds number and surface/gas temperature ratio constant. The air properties used in the work described in this Report do not agree exactly with those in Ref. 3, especially the thermal conductivity values. However, even when the quoted results from Ref. 3 are altered (as far as is possible with the data given) so that they are based on the air properties of Ref. 8, the general conclusion remains that the Nusselt number falls with increased temperature, other parameters being kept constant.

The data obtained in the present work at 600 deg K gas temperature are so scanty and of such poor quality that it is not possible to support or disprove this conclusion, and regrettably, the need for more accurate heat transfer data at higher temperature levels must still remain.

As stated in Appendix II, on two of the test sections static pressure tappings were provided, primarily to enable estimates to be made of the mean density and Mach number in the tubes. Attempts were made to obtain friction factor data from these pressure measurements, but there was considerable scatter on the results, and to have improved them would have required the provision of a series of static pressure tappings along the heated portion and the use of a sensitive

manometer to measure pressure differences. Since the primary object of the test was to obtain heat transfer data, it was thought that this extra complication would not be worthwhile and, further, the tubes from the pressure tappings might constitute another source of heat loss.

6.3. *Correlation of Heat Transfer Data on a Film Temperature Basis.* In order to eliminate terms of the form $(T_s/T_b)^m$ from the modified version of Equation (6), it has become usual for many investigators to define gas properties at some arbitrary film temperature T_f such that

$$T_f = T_b + x(T_s - T_b) \tag{7}$$

where x usually has some value between zero and unity. When measured values of the index m are available, it is possible to deduce values for x if the gas properties are assumed to be proportional to some power of the absolute temperature. It is shown in Appendix IV that if Equation (6) can be expressed with no temperature ratio term and all the gas properties evaluated at some film temperature, then when the gas properties are converted to the bulk values, the following equation results

$$Nu_b = C\,Re_b^{0\cdot8}\,Pr_b^{0\cdot4}\left(\frac{T_f}{T_b}\right)^n \tag{8}$$

where n depends upon the rate at which the gas properties vary with temperature and C is a constant, usually $0\cdot023$. Since the experimental results are expressed in the form

$$Nu_b = C\,Re_b^{0\cdot8}\,Pr_b^{0\cdot4}\left(\frac{T_s}{T_b}\right)^m \tag{9}$$

it follows that

$$\left(\frac{T_s}{T_b}\right)^m = \left(\frac{T_f}{T_b}\right)^n = \left\{1 + x\left(\frac{T_s}{T_b} - 1\right)\right\}^n. \tag{10}$$

The values of m and n are obtained from the experiments and the known variations of gas properties respectively, so that x can be calculated from Equation (10). The values of n are deduced in Appendix IV, so that the following table is obtained

TABLE 3

Gas	m*	n	x
Air ..	−0·40	−0·56	0·7
Helium ..	−0·185	−0·73	0·25
CO_2 ..	−0·27	−0·252	1·0
Argon ..	−0·43	−0·65	0·65

It is obvious that the definition of film temperature varies considerably from one gas to another and this seems to detract from the usefulness of the film temperature concept.

* Since m varies with Reynolds number, an average value is taken for the range of Reynolds numbers above 10,000.

6.4. *Correlation of the Heat Transfer on a Film Temperature and a Film Velocity Basis.* It is possible to carry the analysis one stage further and to define the Reynolds number with the velocity at the point where the fluid temperature is T_f, whence, from Appendix IV, the heat transfer equation becomes

$$Nu_b = C\,Re_b^{0\cdot8}\,Pr_b^{0\cdot4}\left(\frac{T_f}{T_b}\right)^n\left(\frac{U_f}{U_b}\right)^{0\cdot8}. \tag{11}$$

For turbulent flow, with Prandtl numbers near unity, the temperature profile (expressed in terms of $(T_s-T)/(T_s-T_b)$) is very similar to the velocity profile (expressed in terms of U/U_b).

$$Nu_b = C\,Re_b^{0\cdot8}\,Pr_b^{0\cdot4}\left(\frac{T_f}{T_b}\right)^n\left(\frac{T_s-T_f}{T_s-T_b}\right)^{0\cdot8} \tag{12}$$

$$= C\,Re_b^{0\cdot8}\,Pr_b^{0\cdot4}\left(1+x\left(\frac{T_s}{T_b}-1\right)\right)^n(1-x)^{0\cdot8}. \tag{13}$$

Once again the experimental results can be used to obtain values for x. Inspection of Equation (13) shows that x itself must vary with T_s/T_b, and must have a value of zero at unity temperature ratio. Table 4 gives the values of x at $T_s/T_b = 2$.

TABLE 4

Gas	n	$\frac{Nu_b \text{ at temperature ratio } = 2}{Nu_b \text{ at temperature ratio } = 1}$	x
Air ..	−0·56	0·758	0·2
Helium ..	−0·73	0·88	0·08
CO_2 ..	−0·252	0·83	0·17
Argon ..	−0·65	0·743	0·2

The agreement between the values of x is better, and as a first approximation, x could be expressed in terms of T_s/T_b as

$$x = 0\cdot2\left(\frac{T_s}{T_b}-1\right) \tag{14}$$

so that Equation (13) becomes

$$Nu_b = C\,Re_b^{0\cdot8}\,Pr_b^{0\cdot4}\left(1+0\cdot2\left(\frac{T_s}{T_b}-1\right)^2\right)^n\left(1-0\cdot2\left(\frac{T_s}{T_b}-1\right)\right)^{0\cdot8}. \tag{15}$$

It seems reasonable that x should vary with T_s/T_b and that the chosen film conditions should approach those at the surface as T_s/T_b is increased because of the changes described in the temperature profiles, which also apply to the velocity profiles. The formula given as Equation (15) is cumbersome, but if C is put equal to 0·023, it does correlate the data reasonably well, even for helium at temperature ratios up to 1·5, as shown by comparison of Figs. 5, 6, 7 and 8 with Table 5.

TABLE 5

	$\frac{T_s}{T_b}$	1	1·25	1·5	1·75	2·0
Air	$\frac{Nu_b}{Re_b^{0\cdot8}\,Pr_b^{0\cdot4}}$	0·023	0·0219	0·0205	0·0190	0·0174
Helium	$\frac{Nu_b}{Re_b^{0\cdot8}\,Pr_b^{0\cdot4}}$	0·023	0·0219	0·0204	—	—
CO_2	$\frac{Nu_b}{Re_b^{0\cdot8}\,Pr_b^{0\cdot4}}$	0·023	0·022	0·0209	0·0196	0·0183
Argon	$\frac{Nu_b}{Re_b^{0\cdot8}\,Pr_b^{0\cdot4}}$	0·023	0·0219	0·0205	0·0188	0·0171

This sort of treatment can be continued, with more sophisticated expressions for x in terms of T_s/T_b in order to obtain better agreement. However the whole approach remains empirical and any correlation can only apply to a fairly narrow band of Reynolds numbers (because the experimental index m appears to vary with Re_b).

It is felt that a sounder method is to disregard film temperature correlations and to use data in graphical form, wherever possible, or to use a form of Equation (6a), especially for design work, with the values of the constant C and the index m specially chosen to suit the Reynolds number range under consideration.

7.0. *Conclusions.* 1. The effect on surface to gas heat transfer rates of the radial variation of gas properties has been measured for the turbulent flow at low Mach numbers of air, helium, carbon dioxide and argon in smooth circular tubes under conditions of fully developed velocity and temperature profiles.

2. For air, helium and carbon dioxide, the results are presented in a graphical form suitable for design work: alternatively in the Reynolds number range from 10,000 to 20,000 an equation of the following form can be used with all gas properties evaluated at the gas bulk total temperature:

$$Nu_b = 0{\cdot}023 Re_b^{0\cdot8}\, Pr^{0\cdot4} \left(\frac{T_s}{T_b}\right)^m$$

where m has the values $-0{\cdot}4$, $-0{\cdot}185$ and $-0{\cdot}27$ for air, helium and carbon dioxide respectively, in the gas temperature range from 300 deg K to 400 deg K.

3. The reduction in heat transfer coefficient under conditions of constant bulk Reynolds number and gas bulk temperature as the surface temperature rises is probably caused by a reduction of the relative temperature gradient in the 'thermal' laminar sub-layer, which is not fully compensated by the increased thermal conductivity in the laminar sub-layer region.

4. It is concluded that correlation of heat transfer data on a film temperature basis is unsound and that it is better to use data in a graphical form if possible, or in the form of an equation such as is given in Conclusion (2).

5. It cannot be definitely stated whether the constant '0·023' in Conclusion (2) is invariant with temperature level or not. Tests with gases preheated to 600 deg K indicate that it does not deviate very appreciably, if at all, at that temperature.

Acknowledgement. The author would like to acknowledge the help of Mr. J. D. Jackson of the Department of Mechanical Engineering, Manchester University, during part of the experimental work and during numerous discussions on theoretical aspects of the subject.

REFERENCES

No.	Author	Title, etc.
1	D. G. Ainley	Internal air cooling for turbine blades. A general design survey. A.R.C. R. & M. 3013. March, 1955.
2	J. F. Barnes	The calculation of gas flow passage sizes in heat exchangers and nuclear reactors when the heat transfer requirements and the gas inlet and outlet temperatures are specified. A.R.C. 21,499. August, 1959.
3	L. V. Humble, W. H. Lowdermilk and L. G. Desmon.	Measurements of average heat transfer and friction coefficients for subsonic flow of air in smooth tubes at high surface and fluid temperatures. N.A.C.A. Report No. 1020. 1951.
4	Purdue University	Project Squid Semi-Annual Progress Report. April, 1956.
5	R. G. Deissler	Analytical investigation of turbulent flow in smooth tubes with heat transfer with variable fluid properties for Prandtl number of 1. N.A.C.A. Tech. Note 2242. December, 1950.
6	R. G. Deissler and C. S. Eian ..	Analytical and experimental investigation of fully developed turbulent flow of air in a smooth tube with heat transfer with variable fluid properties. N.A.C.A. Tech. Note 2629. February, 1952.
7	J. F. Barnes	Unpublished M.o.A. Report.
8	A. W. Nicklin	The thermal properties of carbon dioxide, nitrogen, air, hydrogen and helium. U.K.A.E.A. (Industrial Group) Tech. Note 36.
9	W. C. Reynolds, W. M. Kays and S. J. Kline.	Heat transfer in the turbulent incompressible boundary layer. III. Arbitrary wall temperature and heat flux. N.A.S.A. Memo. 12-3-58W. (T.L. 6334). December, 1958.
10	J. Hilsenrath and Y. S. Toloukian ..	The viscosity, thermal conductivity, and Prandtl number for air, O_2, NO, H_2, CO, CO_2, H, O, He and A. Trans. A.S.M.E. Vol. 76. pp. 967. 1954. (Alternatively: Tables of properties of gases. U.S. Department of Commerce, National Bureau of Standards. Circular 564. 1st November, 1955.)
11	J. Kaye and J. Keenan	*Thermodynamic properties of air.* John Wiley and Sons Inc., 1945.
12	M. F. Taylor and T. A. Kirchgessner	Measurements of heat transfer and friction coefficient for helium flowing in a tube at surface temperatures up to 5,900 deg R. N.A.S.A. TN D-133. October, 1959.
13	J. D. Jackson	A theoretical Investigation into the effects of surface/gas temperature ratio for fully developed turbulent flow of air, helium, and carbon dioxide in smooth circular tubes. A.R.C. 22,784. April, 1961.

APPENDIX I

Notation and Discussion of Gas Properties

C	Constant in Equation (6)	
Cp	Gas specific heat at constant pressure	C.h.u./lb deg C
D	Diameter of pipe	ft
H	Heat energy dissipated per second in a length of the pipe wall	C.h.u./sec
L	Length of pipe	ft
M	Mach number	
$Nu_b\left(\frac{hD}{\lambda_b}\right)$	Nusselt number with thermal conductivity evaluated at the bulk temperature	
$Pr_b\left(\frac{\mu_b Cp_b}{\lambda_b}\right)$	Prandtl number with gas properties evaluated at the bulk temperature	
Q	Gas mass flow	lb/sec
$Re_b\left(\frac{4Q}{\pi D\mu_b}\right)$	Reynolds number based on mass flow and viscosity at the bulk temperature	
T	Gas total temperature	deg K
$T_b = \frac{1}{QCp}\int_0^{r_i} 2\pi r\rho CpUTdr$.	Bulk gas total temperature ('bulk temperature')	deg K
T_f	Film temperature	deg K
T_s	Surface temperature on the inside of the pipe wall	deg K
T_w	Outside temperature of the pipe wall	deg K
U	Velocity	ft/sec
h	Heat transfer coefficient	C.h.u./sec deg C ft^2
k	Thermal conductivity of pipe wall material	C.h.u./sec deg C ft
m	Experimental index used in Equation (6a)	
n	Theoretical index defined in Appendix IV	
q	Heat flux	C.h.u./ft^2 sec
r	Pipe radius	ft

r_i	Inside radius of pipe wall	ft
r_0	Outside radius of pipe wall	ft
r^+	Dimensionless pipe radius defined in Appendix III	
t^+	Dimensionless gas temperature (Appendix III)	
u^+	Dimensionless velocity (Appendix III)	
x	Fraction defined in Equation (7)	
y	Distance from the pipe wall	ft
y^+	Dimensionless distance (Appendix III)	
α	Index for variation of viscosity with temperature	
β	Index for variation of thermal conductivity with temperature or Heat loading parameter defined in Appendix III	
γ	Ratio of gas specific heats at constant pressure and constant volume	
δ	Index for variation of specific heat with temperature	
ϵ	Mechanical diffusivity	ft^2/sec
ϵ_h	Thermal diffusivity	ft^2/sec
λ	Gas thermal conductivity	C.h.u./ft sec deg C
μ	Gas viscosity	lb/ft sec
ν	Kinematic viscosity	ft^2/sec
ρ	Gas density	lb/ft^3
τ	Shear stress	$poundals/ft^2$

Suffices

b	Bulk value, or Evaluated at bulk conditions
f	Film value or Evaluated at film conditions
s	Surface value or Evaluated at surface conditions

Gas Properties

Nicklin[8] surveys the properties of some commonly used gases and gives graphs showing the variations of these properties with temperatures up to about 1,000 deg K.

Hilsenrath and Toloukian[10] have carried out what appears to be the most complete and up to date survey of gas properties and this includes tables of values and an extensive discussion of previous work and the reliability of the results. Comparison of Refs. 8 and 10 for properties of air, helium and carbon dioxide shows that the agreement between the two sets of data is very good. Ref. 8 happened to be a convenient source of data for computation of heat transfer results and was therefore used for these three gases. For argon, Ref. 10 had to be used in the absence of any other data. The gas properties used in Ref. 3 are based on Keenan and Kaye[11] up to 500 deg K, and for higher temperatures extrapolated values of thermal conductivity are quoted. At 500 deg K the values of Ref. 11 are about $1\frac{1}{2}$ per cent higher than the more recent values of Ref. 10. At 1,000 deg K, the extrapolated thermal conductivity values of Ref. 3 are 5 per cent higher than those quoted in Ref. 10.

APPENDIX II

Description of Apparatus

General. Previous work[7] had demonstrated the feasibility of the technique for measuring Nusselt numbers in the region of the test section where radial velocity and temperature profiles were fully developed. These experiments were performed on a very simple rig using compressed air from the laboratory supply and discharging the heated air to atmosphere. It was obvious however that such a technique would lead to prohibitively high operating costs if used with helium as the working substance, and therefore that a closed cycle apparatus would have to be constructed, with very careful attention paid to the problem of leakage, so that a small quantity of helium could be circulated repeatedly, and only a minute make-up supply would be needed to cope with leakage during operation.

In Fig. 1 a flow diagram of the rig is shown. During normal operation the gas was compressed and passed through a cooler to a receiver. A by-pass control then regulated the proportions of gas passing either *via* an orifice measuring section to the heat transfer test section and/or back to the inlet receiver of the circulating pump. Gas which had been heated in the test section was cooled and passed through a silica gel drier before rejoining the by-pass flow at inlet to the reciprocating compressor, which was a twin cylinder 'oil free' type. The pistons of this compressor had self-lubricating carbon rings and were operated by piston rods which passed through glands. On the other (lower) side of these glands, the piston rods were actuated by normal oil lubricated pistons, and provided the pressure in the chambers above the glands exceeded the atmospheric value by a small amount ($\frac{1}{4}$ lb/in.^{2}) no air or oil could pass up through the glands from the crankcase. Normally any gas which leaked past the pistons would have been allowed to escape, but in this apparatus the compressor was modified to allow most of the leakage to be pumped back through a small diaphragm type compressor to the inlet receiver. The pressure in the chambers above the glands was kept at about $\frac{1}{4}$ lb/in^2 gauge by means of a throttle valve and also by a pressure sensitive switch controlling the motor of the scavenge compressor. Operating the apparatus in this manner and taking care to maintain all the joints between various parts of the rig in as leak-free a condition as possible, experiments were conducted for over thirty hours with a total consumption of 200 cu ft of helium (at N.T.P.). This included having to evacuate and refill the rig on four occasions after changes of orifice plates or test sections.

In order to fill the rig with gas, the scavenge compressor could be made to evacuate the apparatus (excluding the main compressor) by altering certain valves. The rig could then be refilled from the gas supply and the process was repeated, usually three times, when the proportion of contaminant was less than 1 per cent. After each filling, the gas was passed into the main compressor and allowed to discharge to atmosphere through the glands. Special precautions were taken to prevent contamination by water and mercury vapour from manometers during evacuation.

The make-up supply was controlled by a small valve in parallel with the main supply valve which was too coarse for any operation except filling the rig with gas. The total capacity of the rig was approximately 1 cu ft. Also the pressure and density levels in the rig could be altered, so that the average Mach number of the flow in this section could be chosen at the discretion of the operator, provided the pressure did not exceed 100 lb/in.^{2} gauge (the maximum working pressure of the main compressor).

The test section itself was heated electrically, using an alternating current up to 480 amperes, at a potential difference up to 6 volts. The main circuit for this is shown at the top of Fig. 2.

Test Sections. Three test sections were used for the experiments described in this Report, and all three were the same in principle. A detailed description of the first will be given; this section was used for most of the experiments and only the differences between it and subsequent test sections will be mentioned.

Test Section No. 1 consisted of a stainless steel tube, 28 in. long and of $\frac{3}{8}$ in. outside diameter. Its bore was 0·247 in. and was polished. The heated section was 12 in. (48·6 diameters) long and the outside diameter of this portion was turned down to 0·333 in. to give the required electrical resistance. A starting section of approximately 14 in. (57 diameters) was provided and the entry to the tube was sharp edged so that the beginning of the heated section, the velocity profile would be well established. Copper connectors were brazed at each end of the heated portion and two static pressure tappings were welded to the tube, 13 in. apart and on either side of the heated section. The temperatures along the outside of the tube wall were measured by chromel/alumel thermocouples made from 33 S.W.G. wires calibrated at the N.P.L. The thermocouples were fixed to the tube by a resistance welding technique and care was taken to ensure that the wires of any one thermocouple were not connected to the tube at different axial positions. This precaution avoided spurious A.C. voltages from being superimposed on the thermocouple reading. In order to give the thermocouple adequate mechanical strength they were sleeved in woven silica braid and bound by silica thread to the tube as shown in Fig. 3. The thermocouples were connected via switches to a calibrated potentiometer. The positions of the thermocouples over the whole of the heated portion are shown on the lower diagram on Fig. 2, where a specimen temperature distribution is plotted. The close spacing of the thermocouples at each end of the heated section (Fig. 3) enabled conduction losses to be assessed accurately.

The electric current supplied to the tube was measured using an A.C. milliameter and current transformers of 2,000/1 and 4,000/1 ratios, permitting the measurement of currents up to 240 and 480 amperes respectively. The two transformers and the milliameter were checked against a sub-standard instrument. In order to be able to measure the electric power dissipated in various sections of the tube, five chromel voltage tappings were spaced at 3 in. intervals along the tube and a switching arrangement (Fig. 2) enabled the potential difference to be measured between adjacent tappings using a calibrated valve millivoltmeter. This last instrument was chosen because it consumed no current, so that there was no error caused by voltage drops in the leads from the voltage tappings to the instrument.

The static pressure tappings were connected to either a water or a mercury manometer and the upstream tapping was also connected to a pressure gauge. By this means the mean pressure and hence the mean Mach number in the tube could be calculated, if necessary.

The whole tube was placed in a box filled with mica insulation material to minimize heat losses. At each end of the tube a disc of asbestos/cement material was fixed to insulate electrically the test section from the rest of the rig which would otherwise have provided an alternative path for the current. It was necessary to insulate both ends of the tube, otherwise the valve millivoltmeter would have measured a potential relative to earth instead of the potential difference between two points on the tube. The insulating discs were impregnated to render them non-porous and were bolted as shown in Fig. 3a to mixing chambers, which were connected to the rest of the rig by stainless steel piping. The drawing in Fig. 3a shows the outlet end of Test Section No. 1. In order to measure the outlet gas bulk temperature accurately, the mixing device, consisting essentially of a cone with its apex pointing upstream and ventilated by three holes, was located as near as possible

to the end of the heated section. With the small bore tube used for this test section it was evident that with helium the exit Mach numbers would be approaching unity at the upper end of the Reynolds number range so that some means for diffusing the gas would have to be provided before mixing occurred. Fig. 3a shows the device finally evolved. It was made from brass and the diffuser wall thicknesses were made as thin as possible to minimize its thermal capacity. Provision was also made to allow the gas, after its temperature had been measured with the thermocouple, to circulate over the outside walls of the diffusing section. Also a small 150 watt heating element was made from 30 S.W.G. Nichrome wire, sleeved in silica braid and wound upon a brass former. This element was a push fit inside the threaded portion of the brass end piece used to clamp the insulating disc and served to heat the clamping nut which had an unavoidably large thermal capacity. Thermocouples were buried in the brass end piece and the radial wall between the tube and the threaded section was turned down to $\frac{1}{16}$ in. thickness to minimize heat flow either to or from the tube walls. The current to the heater was adjusted by means of a variable auto-transformer so that the two thermocouples embedded in the brass end piece gave readings as close as possible to the observed reading of the thermocouple measuring the gas outlet total temperature. It was found that generally the latter thermocouple responded slowly to changes in the wall temperatures, so that a clear cut reading where all three thermocouples agreed was usually possible. Under steady conditions the power needed to maintain the end piece at constant temperature was very small.

The measurement of the inlet gas temperature was made by a thermocouple situated in a similar mixing chamber upstream of the sharp edged entry. This temperature was rarely more than 1 deg C different from the room temperature for Test Section No. 1.

The electrically heated portion of Test Section No. 2 was exactly twice as long as that of Test Section No. 1. The outside diameter of this tube was $\frac{5}{8}$ in. and the bore was 0·553 in., giving a length/diameter ratio of 43·4 for the heated section. An entry length of approximately equal length was provided, with a sharp entry as before. This tube was used for tests at Reynolds numbers up to 10,000 because it permitted larger mass flows to be used, thus easing the two problems of measuring the small electrical powers which would have been needed with the first test section and of measuring the exit gas temperature. It was no longer necessary to diffuse the gas at the exit; on the contrary it was possible to situate the mixing cone in the bore of the tube itself and at the same time provide a stream of high velocity gas to heat the thermocouple to its equilibrium value. As before, a 150 watt heater was used to maintain the clamping nut and threaded portion at the equilibrium temperature. These two test sections were used to obtain all the data given in the range 300 deg K to 400 deg K.

The third test section was the same size as the first as regards the heated portion, but the connectors were made from stainless steel to reduce conduction losses from the tube to the supply leads. No static pressure tapping was provided. The wall thermocouples and voltage tappings were situated in exactly the same positions as on No. 1 and in addition one wall thermocouple was fixed to the entry section which was situated in a special entry mixing chamber. This allowed the incoming gas from the preheaters to flow over the outside of the entry section before passing the gas inlet thermocouple and flowing into the tube. The entry mixing chamber itself was heated by a 1 kW electrical heater controlled by a variable auto-transformer and thermocouples were situated on the mixing chamber walls. By this means it was possible to adjust conditions so that the inlet section temperature and the inlet gas temperature were in agreement.

At the exit end of the heated section, no diffuser was provided because the helium flow range was restricted to Reynolds numbers around 10,000, and the exit Mach numbers were less than 0·5. Instead there was a sudden enlargement in flow cross section, with the mixing cone fitted in the enlarged portion. The parts for this end piece were made in stainless steel and the discs at either end were also made from $\frac{1}{32}$ in. stainless steel sheet, after many unsuccessful attempts to render the insulating material non-porous at the elevated temperatures (greater than 300 deg C). In order to insulate the heated portion, insulating gaskets were used between the flanges of joints upstream and downstream of the test section and specially bushed bolts with insulating end washers were used. Attempts to use a 150 watt heating element on the exit of the test section were also unsuccessful, because the temperatures involved (greater than 500 deg C) caused failure of the windings. Instead a 500 watt element was wound on the outside of the mixing chamber. In practice it was found that this was needed only during warming up of the rig.

The gas itself was preheated by passing it through four tubes connected in series. In each tube there was a 1 kW electric fire element, again controlled by a variable auto-transformer. The maximum power available was sufficient to preheat helium to a temperature of 600 deg K with a test section Reynolds number of 10,000. The flow connections to the heaters were connected in series for two reasons, in spite of the high pressure loss caused thereby. The first reason was that the overall temperature variation from one end of the heating element to the other was minimized, thus reducing the possibility of failure by thermal stress and the second was that in the event of electrical failure of one or more heaters, the others would not be starved of gas and become overheated. (With heaters in parallel, a sudden electrical failure causes an increase in mass flow through the failed heater because there is no pressure loss due to heat addition, coupled with a fall in mass flow through the remainder, which therefore become hotter.)

APPENDIX III

The Assumptions used in the Derivation of Temperature and Velocity Profiles and their use to deduce Nusselt Numbers as Functions of Reynolds Number and Surface/Gas Temperature Ratio

In Ref. 6, a non-dimensional velocity u^+ and a non-dimensional temperature t^+ are plotted as functions of y^+, a non-dimensional distance from the surface of a pipe of circular cross section, for various values of a heat loading factor β, which is positive for heat addition and negative for heat extraction from the gas. These non-dimensional parameters are defined as

$$u^+ = \frac{U}{\sqrt{(\tau_s/\rho_s)}} \tag{1}$$

$$y^+ = \frac{y\sqrt{(\tau_s/\rho_s)}}{\nu_s} \tag{2}$$

$$t^+ = \frac{1}{\beta}\left(1 - \frac{T}{T_s}\right) \tag{3}$$

$$\beta = \frac{q_s\sqrt{(\tau_s/\rho_s)}}{Cp\tau_s t_s} \tag{4}$$

The velocity and temperature profiles are obtained by converting the following equations for heat and momentum transfer into dimensionless form and integrating them
Heat flux

$$q = -(\lambda + \rho\epsilon_h Cp)\frac{\partial T}{\partial y} \tag{5}$$

Momentum flux

$$\tau = (\mu + \rho\epsilon)\frac{\partial U}{\partial y} \tag{6}$$

Having converted Equations (5) and (6) into dimensionless form it is necessary to specify the variations of shear stress τ and heat flux q across the pipe and to specify the variation of ϵ and ϵ_h with distance from the pipe wall, as well as the boundary conditions. It is also necessary to make assumptions for the variations of gas properties with temperature. These are dealt with in detail in Ref. 6; it is sufficient to state here that shear stress and heat flux were maintained constant and that the variations of ϵ and ϵ_h (assumed equal) were based on experimental data for flow in pipes at $T_s/T_b = 1$. (Also in the analysis it was assumed that the difference between total and static temperatures could be neglected, *i.e.*, low subsonic flow prevailed.)

The data are presented as graphs of u^+ and t^+ plotted against y^+ for constant values of β. For any chosen values of r^+ (the dimensionless quantity corresponding to the pipe radius) and β it is possible to perform integrations by numerical methods to obtain $u_b{}^+$ and $t_b{}^+$
where

$$u_b{}^+ = \frac{2}{(r^+)^2}\int_0^{r+} u^+(r^+ - y^+)dy^+ \tag{7}$$

and

$$t_b{}^+ = \frac{\displaystyle\int_0^{r+} \frac{t^+u^+(r^+ - y^+)}{1 - \beta t^+}\,dy^+}{\displaystyle\int_0^{r+} \frac{u^+(r^+ - y^+)}{1 - \beta t^+}\,dy^+} \tag{8}$$

Having obtained u_b^+ and t_b^+, it is shown in Ref. 5 that

$$Nu_b = \frac{2r^+ Pr}{t_b^+}\left(\frac{T_s}{T_b}\right)^{0\cdot68} \tag{9}$$

and

$$Re_b = 2u_b^+ r^+ \left(\frac{T_s}{T_b}\right)^{1\cdot68} \tag{10}$$

where

$$\frac{T_s}{T_b} = \frac{1}{(1-\beta t_b^+)} \tag{11}$$

(viscosity and thermal conductivity are both assumed to be proportional to $(T)^{0\cdot68}$). The definition of Re_b given above is consistent with that used in the experimental work, *viz.*,

$$Re_b = \frac{4Q}{\pi D\mu_b} \tag{12}$$

It follows that having chosen r^+ and β, the values of Nu_b, T_s/T_b and Re_b follow as a result of the calculation so that some trial and error is necessary if particular values of T_s/T_b and Re_b are specified. This is why the quantities in Figs. 13, 14 and 16 have the values quoted. Having obtained the conditions which give the desired Re_b and T_s/T_b, the velocity profiles can be obtained easily as functions of y/r using the following equations

$$\frac{y}{r} = \frac{y^+}{r^+} \tag{13}$$

$$\frac{U}{U_b} = \frac{u^+}{u_b^+} \tag{14}$$

$$\frac{T_s - T}{T_s - T_b} = \frac{t^+}{t_b^+} \tag{15}$$

As an alternative approach to deducing values of Nu_b as functions of Re_b and T_s/T_b from the Equations (9), (10) and (11), it is interesting to consider the heat flux in the laminar sub-layer, where, by definition

$$q_s = -\lambda_s\left(\frac{\partial T}{\partial y}\right)_s \tag{16}$$

or

$$q_s = +\lambda_b\left(\frac{\lambda_s}{\lambda_b}\right)\left(\frac{\partial}{\partial y}(T_s - T)\right)_s \tag{17}$$

so that

$$Nu_b = \frac{2rq_s}{\lambda_b(T_s - T_b)} = 2\left(\frac{\lambda_s}{\lambda_b}\right) r\left(\frac{\partial}{\partial y}\left(\frac{T_s - T}{T_s - T_b}\right)\right)_s \tag{18}$$

or

$$Nu_b = 2\left(\frac{T_s}{T_b}\right)^{0\cdot68}\frac{r^+}{t_b^+}\left(\frac{\partial t^+}{\partial y^+}\right)_s . \tag{18a}$$

By re-writing Equation (16) in dimensionless form it is possible to show, for the region near the wall, *i.e.*, $(0 \leqslant y^+ \leqslant 5)$,
that

$$\left(\frac{\partial t^+}{\partial y^+}\right)_s = Pr \tag{19}$$

Substituting from Equation (19) into Equation (18a) and using the fact that Pr is assumed to be $0{\cdot}73$, we obtain a relation which is identical with Equation (9) (as would be expected) *i.e.*,

$$Nu_b = 1{\cdot}46 \left(\frac{T_s}{T_b}\right)^{0{\cdot}68} \frac{r^+}{t_b^+} \tag{20}$$

However, this second method of deducing Nu_b provides a physical explanation of the observed and calculated temperature ratio effects at a constant bulk Reynolds number. Nu_b falls because the temperature profiles in the laminar sub-layer as shown on Figs. 13 and 14 become less steep, relative to the pipe radius, as T_s/T_b is increased. This reduction in gradient is counteracted to some extent by the increase in thermal conductivity near the wall, relative to the bulk value. It is reasonable to expect that, for different gases, there will be different changes of sub-layer temperature profile and thermal conductivity and therefore the influence of changes in surface/gas temperature ratio will not be the same.

The assumptions made in Ref. 6 apply most closely to helium, and from Fig. 9 as T_s/T_b is increased from 1 to $1{\cdot}6$, at $Re_b = 11{,}800$, $Nu_b/(Pr_b)^{0{\cdot}4}$ falls from 42 to 37, so that the ratio of the respective Nusselt numbers is 37/42, *i.e.*, $0{\cdot}88$, neglecting any small change in $(Pr_b)^{0{\cdot}4}$ (Fig. 4).

From Fig. 13, for $Re_b = 11{,}800$, $r_0^+ = 200$ at $T_s/T_b = 1{\cdot}58$, and at $y^+ = 5$, $y/r = 0{\cdot}025$

$$\frac{T_s - T}{T_s - T_b} = 0{\cdot}295,$$

so

$$r\left(\frac{\partial}{\partial y}\left(\frac{T_s - T}{T_s - T_b}\right)\right)_s = \frac{0{\cdot}295}{0{\cdot}025} = 11{\cdot}8$$

Similarly at $T_s/T_b = 1$, $r^+ = 360$, and at $y^+ = 5$, $(y/r = 0{\cdot}0139)$

$$\frac{T_s - T}{T_s - T_b} = 0{\cdot}248,$$

so

$$r\left(\frac{\partial}{\partial y}\left(\frac{T_s - T}{T_s - T_b}\right)\right)_s = \frac{0{\cdot}248}{0{\cdot}0139} = 17{\cdot}85$$

The ratio of the respective Nusselt numbers is therefore, using Equation (18)

$$\frac{Nu_1}{Nu_2} = \frac{(1{\cdot}58)^{0{\cdot}68} \times 11{\cdot}8}{17{\cdot}85}$$

$$= 1{\cdot}365 \times 0{\cdot}66$$

$$= 0{\cdot}90 \text{ which is in fair agreement with the experimental value.}$$

APPENDIX IV

Correlation of Heat Transfer Data at an Arbitrary Film Temperature

Suppose that the Nusselt number, Reynolds number and Prandtl number in Equation (6) (Section 5.0) are defined with gas properties taken at some arbitrarily selected temperature so that no temperature ratio term need be included; *i.e.*,

$$Nu_f = \frac{hD}{\lambda_f} = C\left(\frac{\rho_f UD}{\mu_f}\right)^{0\cdot8}\left(\frac{\mu_f Cp_f}{\lambda_f}\right)^{0\cdot4} \tag{1}$$

Then

$$Nu_b = \frac{hD}{\lambda_b} = \frac{hD}{\lambda_f}\frac{\lambda_f}{\lambda_b}$$

$$= C\,Re_b^{0\cdot8}\,Pr_b^{0\cdot4}\left(\frac{\rho_f}{\rho_b}\right)^{0\cdot8}\left(\frac{\mu_b}{\mu_f}\right)^{0\cdot4}\left(\frac{\lambda_f}{\lambda_b}\right)^{0\cdot6}\left(\frac{Cp_f}{Cp_b}\right)^{0\cdot4} \tag{2}$$

when the bulk values are used to define the dimensionless parameters.

If it is assumed that

$$\rho \propto T^{-1}$$

$$\mu \propto T^{\alpha}$$

$$\lambda \propto T^{\beta}$$

$$Cp \propto T^{\delta}$$

then

$$Nu_b = C\,Re_b^{0\cdot8}\,Pr_b^{0\cdot4}\left(\frac{T_f}{T_b}\right)^{n}, \tag{3}$$

where

$$n = -0\cdot8 - 0\cdot4\alpha + 0\cdot6\beta + 0\cdot4\delta. \tag{4}$$

For the four gases considered the following table gives the values of α, β, δ and n.

Gas	α	β	δ	n
Air ..	0·6924	0·7954	0·0875	−0·565
Helium ..	0·6822	0·5775	0	−0·726
CO_2 ..	0·8214	1·2440	0·3250	−0·252
Argon ..	0·7265	0·7320	0	−0·651

The above data are based on Ref. 10, over the range 300 deg K to 900 deg K. Ref. 8, on which the experimental data are based, agrees well with Ref. 10 in the temperature range 300 deg K to 600 deg K.

When the Reynolds number is based on a film velocity also, *i.e.*,

$$Re_f = \frac{\rho_f U_f D}{\mu_f} \tag{5}$$

and it is assumed that an equation of the form

$$Nu_f = C\, Re_f^{0\cdot8}\, Pr_f^{0\cdot4} \tag{6}$$

is independent of temperature ratio effects, conversion of this Equation (6) to bulk values gives

$$Nu_b = C\, Re_b^{0\cdot8}\, Pr_b^{0\cdot4} \left(\frac{T_f}{T_b}\right)^n \left(\frac{U_f}{U_b}\right)^{0\cdot8} \tag{7}$$

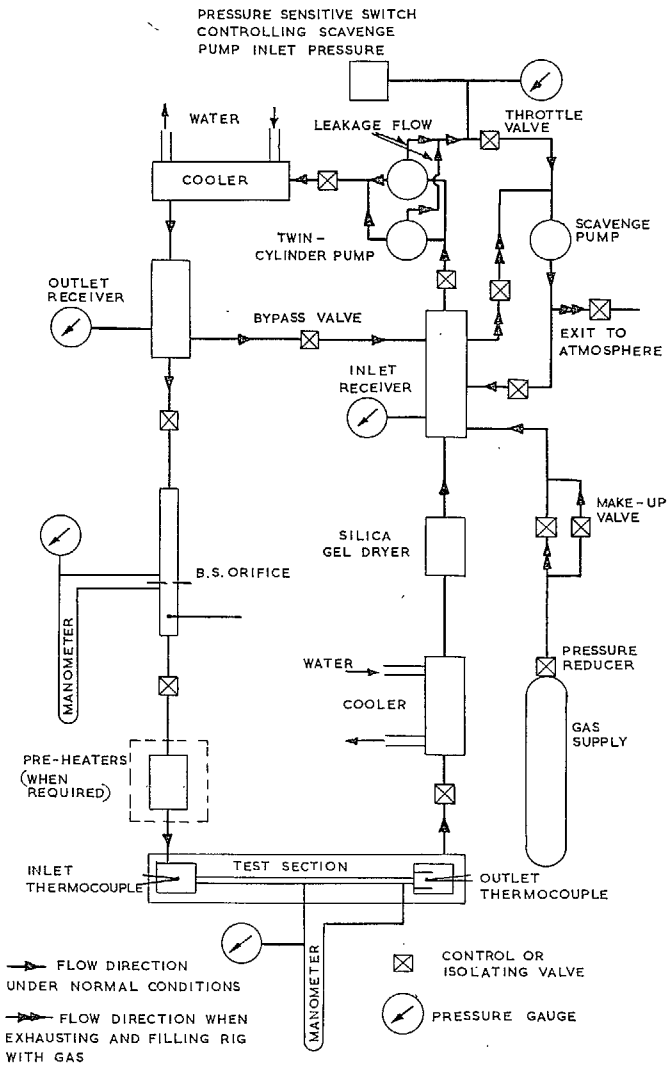

FIG. 1. Gas flow diagram.

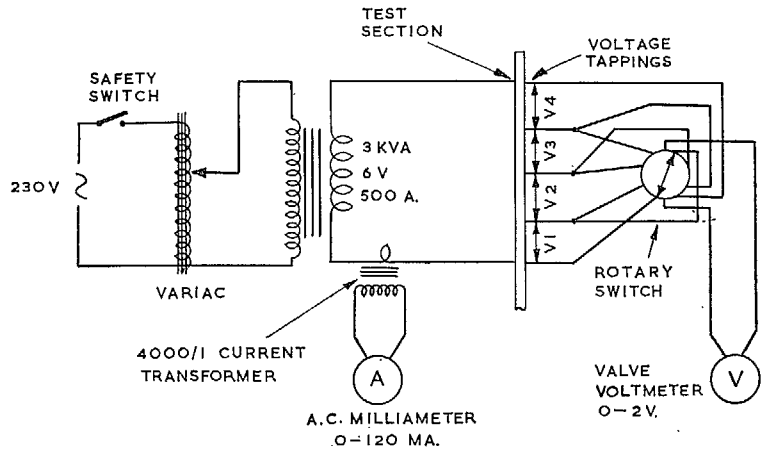

FIG. 2a. Test Section main electrical circuit.

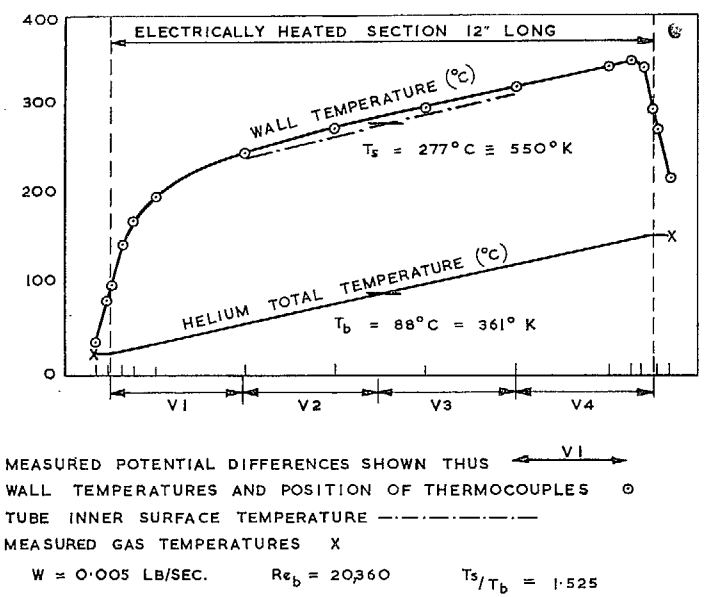

FIG. 2b. Typical temperature distributions.

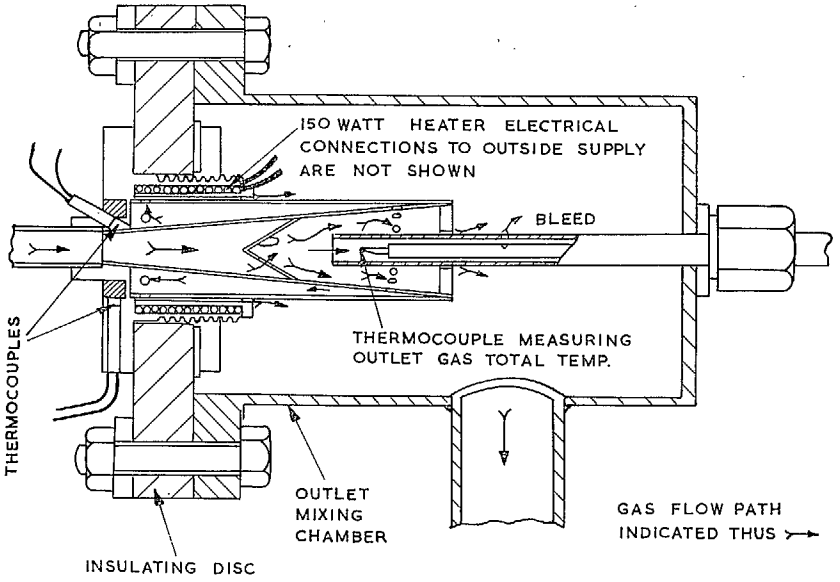

FIG. 3a. Details of exit diffuser and mixer for Test Section No. 1.

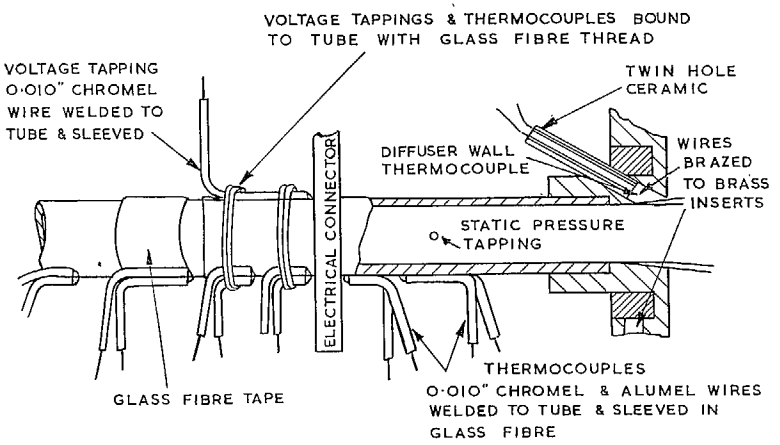

FIG. 3b. Details of wall thermocouples on Test Section No. 1.

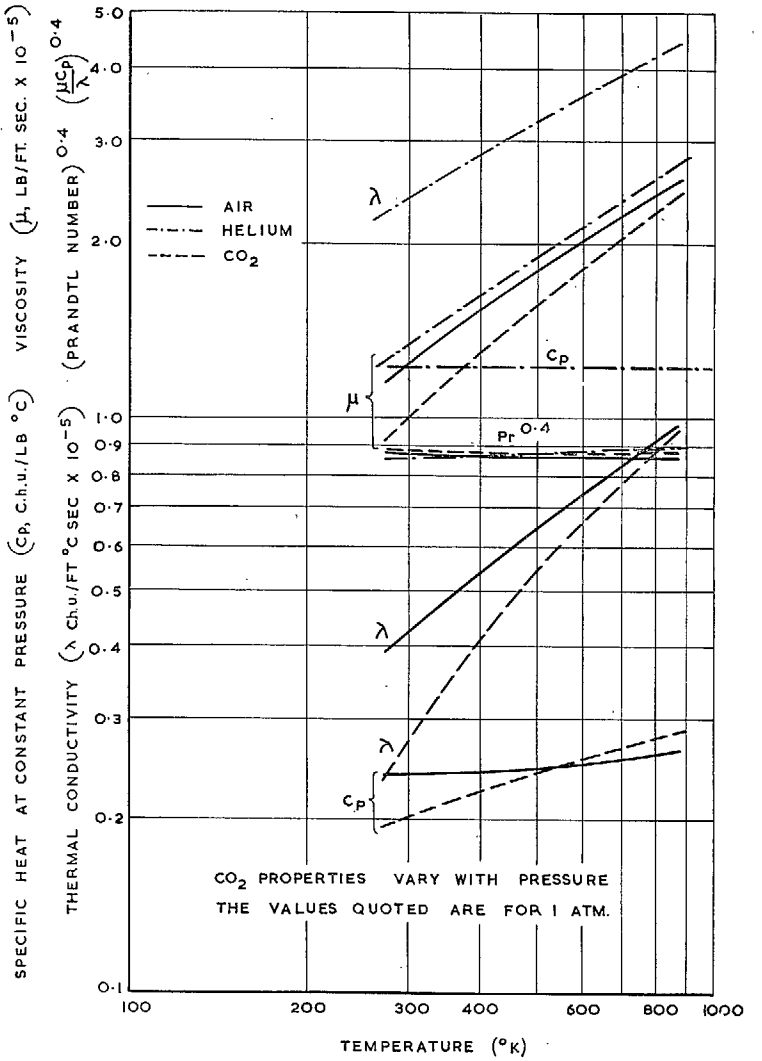

FIG. 4. Gas properties. (Air, helium and carbon dioxide.) Ref. 8.

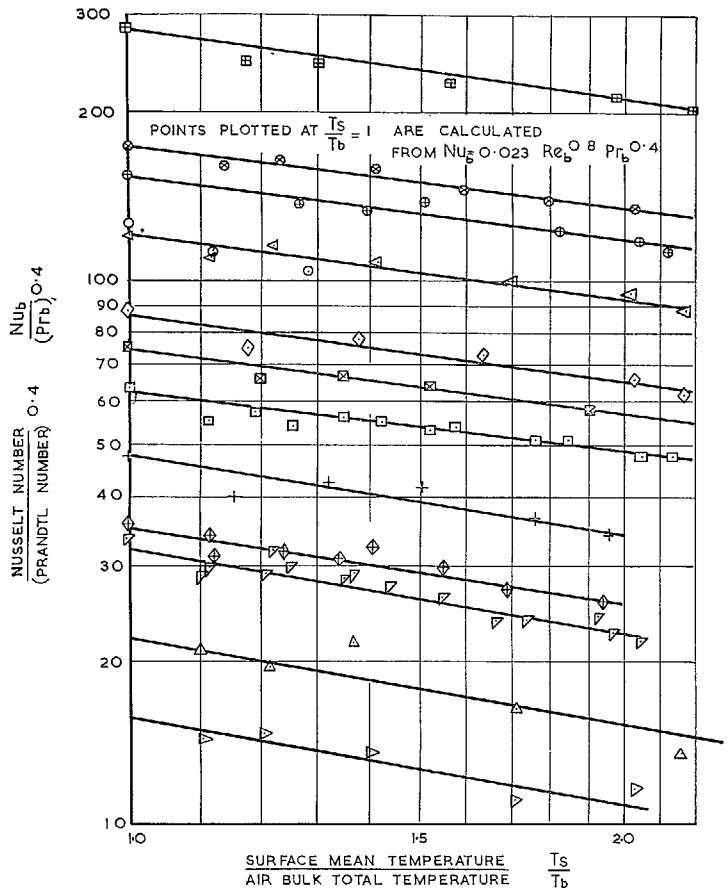

KEY TO SYMBOLS

REYNOLDS No.	REYNOLDS No.	REYNOLDS No.
⊞ 130,000	◇ 30,000	▽ 9,000
⊗ 70,000	⊠ 25,000	△ 6,000
⊕ 60,000	⊡ 20,000	▷ 4,200
⊙ 47,000	+ 14,000	
◁ 45,000	◈ 10,000	

FIG. 5. Experimental heat transfer results for air with all gas properties evaluated at *Tb*.
(300 *deg*. $K < Tb <$ 400 *deg*. K : $Re_b > 4000$.)

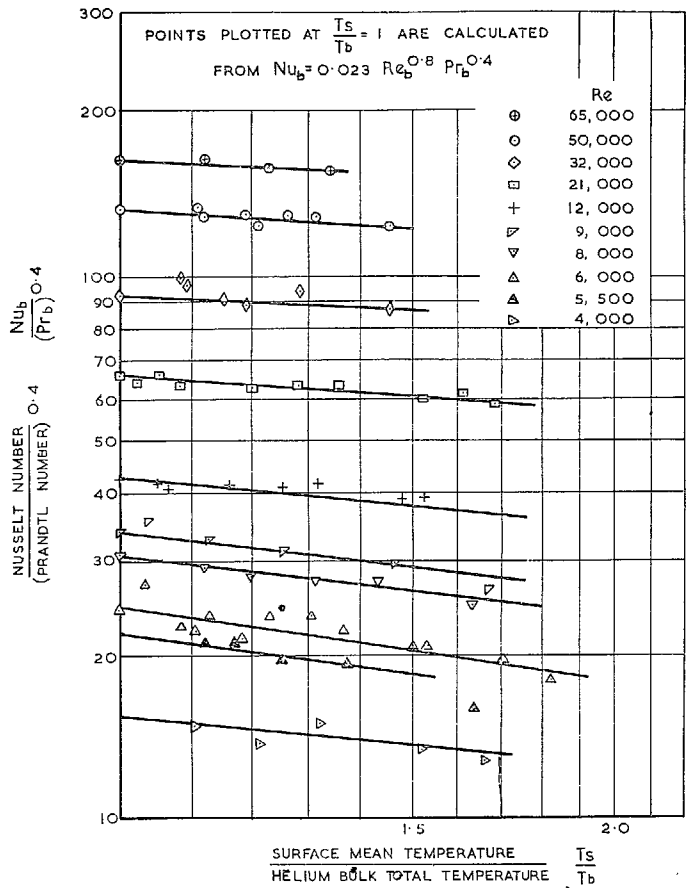

FIG. 6. Experimental heat transfer results for helium with all gas properties evaluated at *Tb*.
(300 *deg*. $K < Tb <$ 400 *deg*. K : $Re_b > 4000$.)

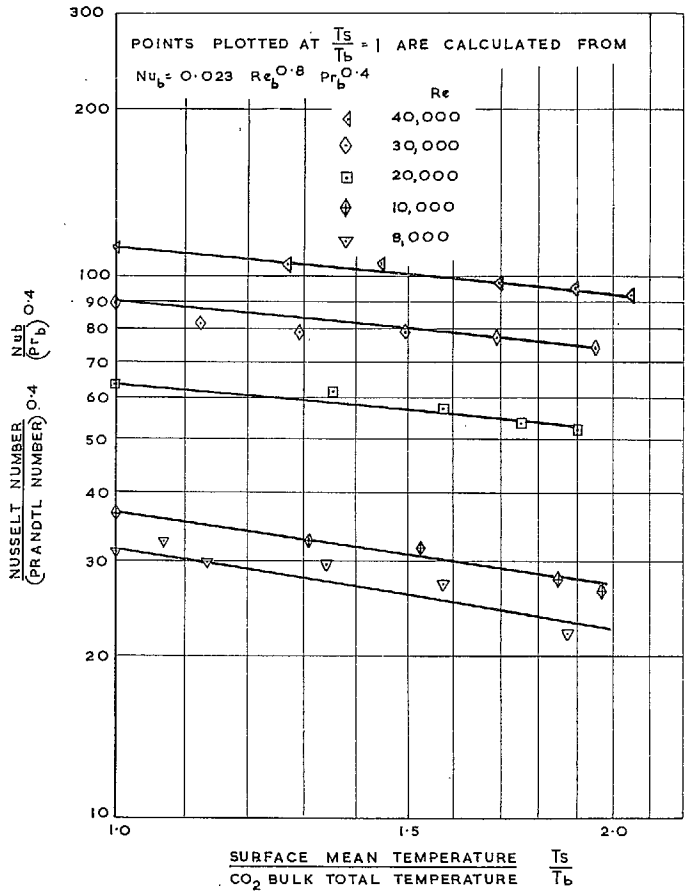

FIG. 7. Experimental heat transfer results for carbon dioxide with all gas properties evaluated at *Tb*.
(300 *deg. K* < *Tb* < 400 *deg. K* : $Re_b \geqslant 8000$.)

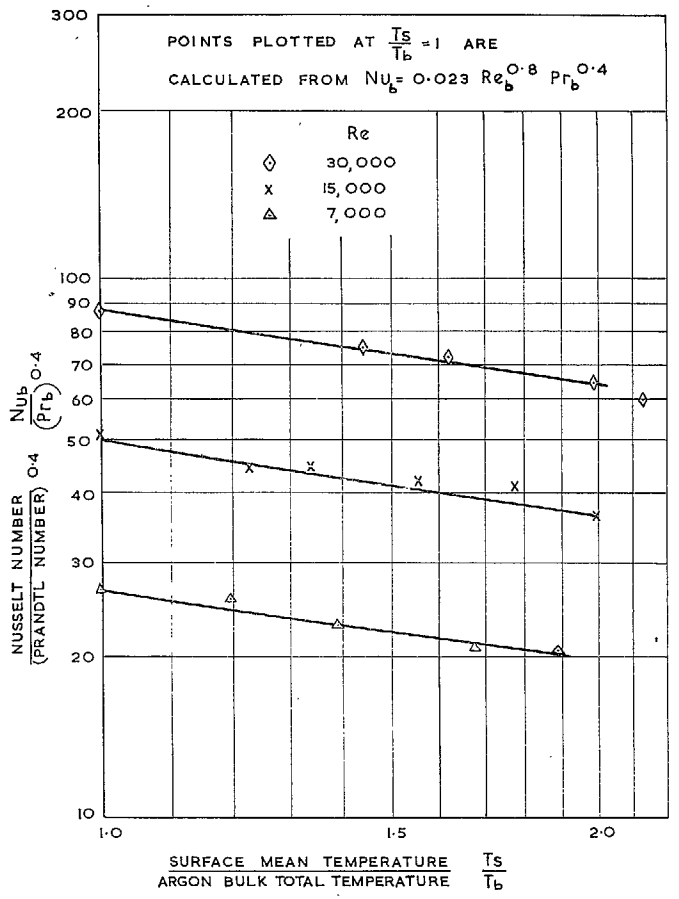

FIG. 8. Experimental heat transfer results for argon with all gas properties evaluated at T_b.
(300 *deg. K* < T_b < 400 *deg. K* : $Re_b \geqslant 7000$.)

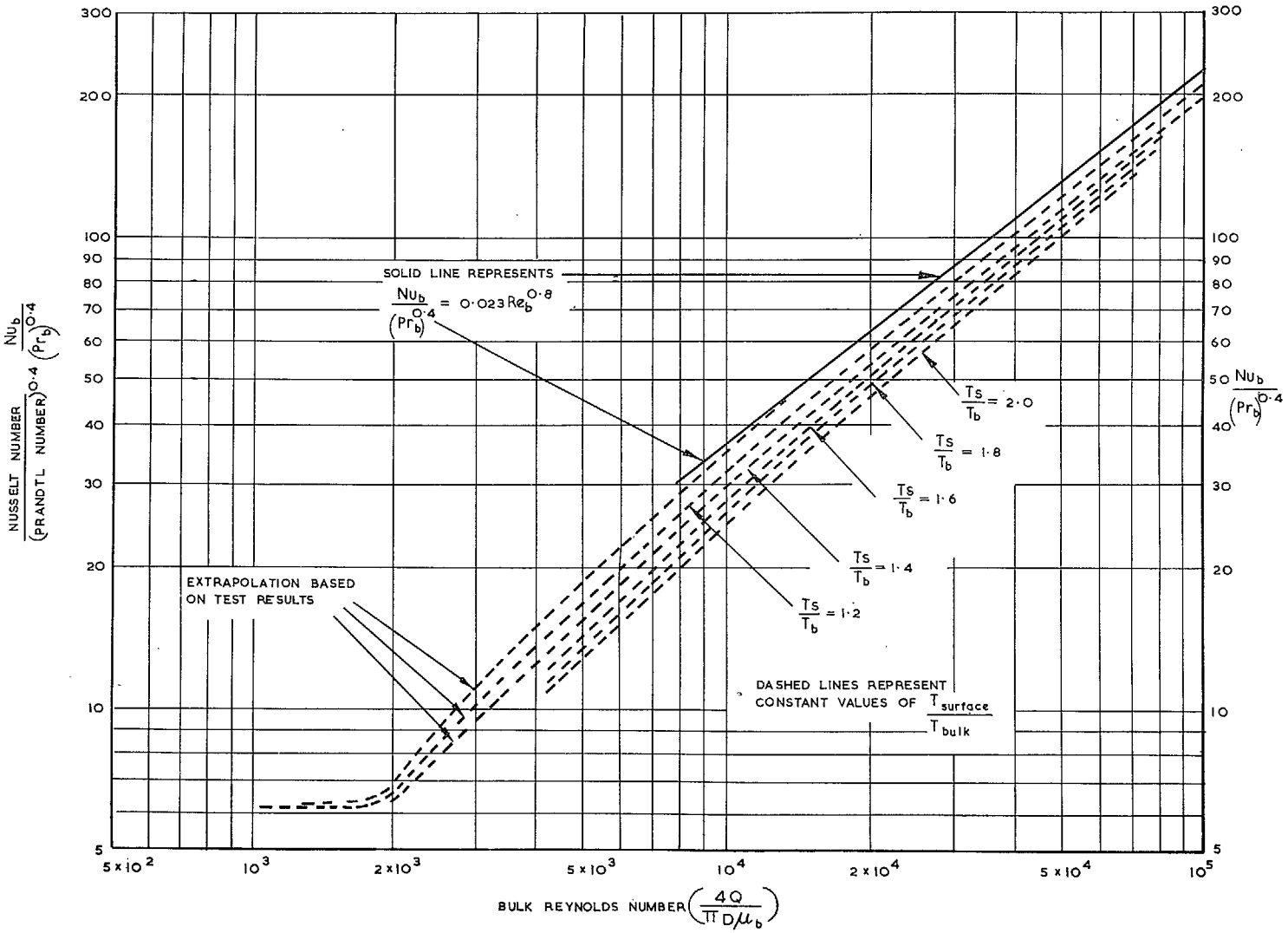

FIG. 9. Summary of air heat transfer results with all gas properties evaluated at T_b. (300 *deg.* $K < T_b <$ 400 *deg.* K) and (300 *deg.* $K < T_s <$ 700 *deg.* K).

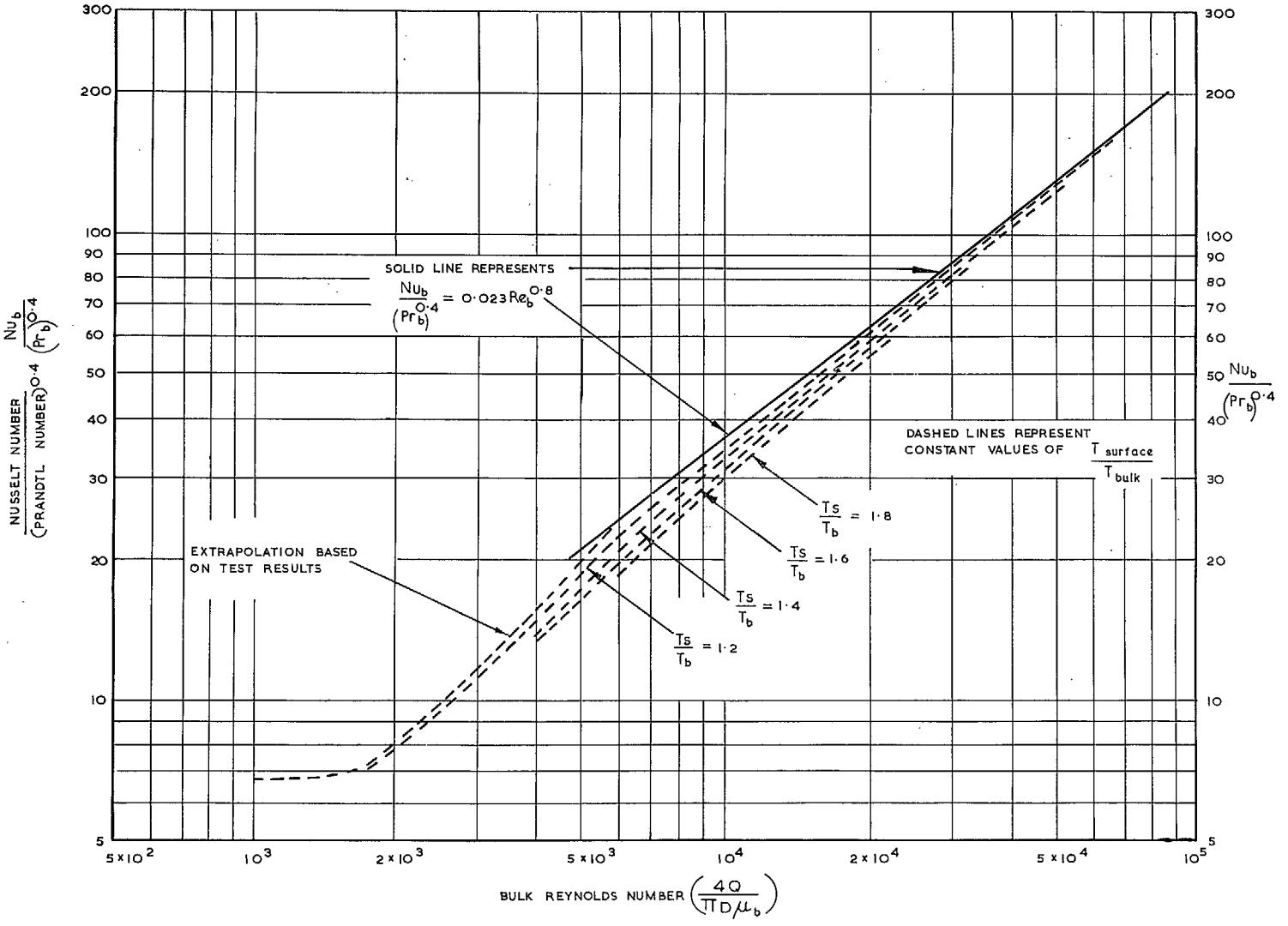

FIG. 10. Summary of helium heat transfer results with all gas properties evaluated at T_b. (300 *deg.* $K < T_b <$ 400 *deg.* K) and (300 *deg.* $K < T_s <$ 700 *deg.* K).

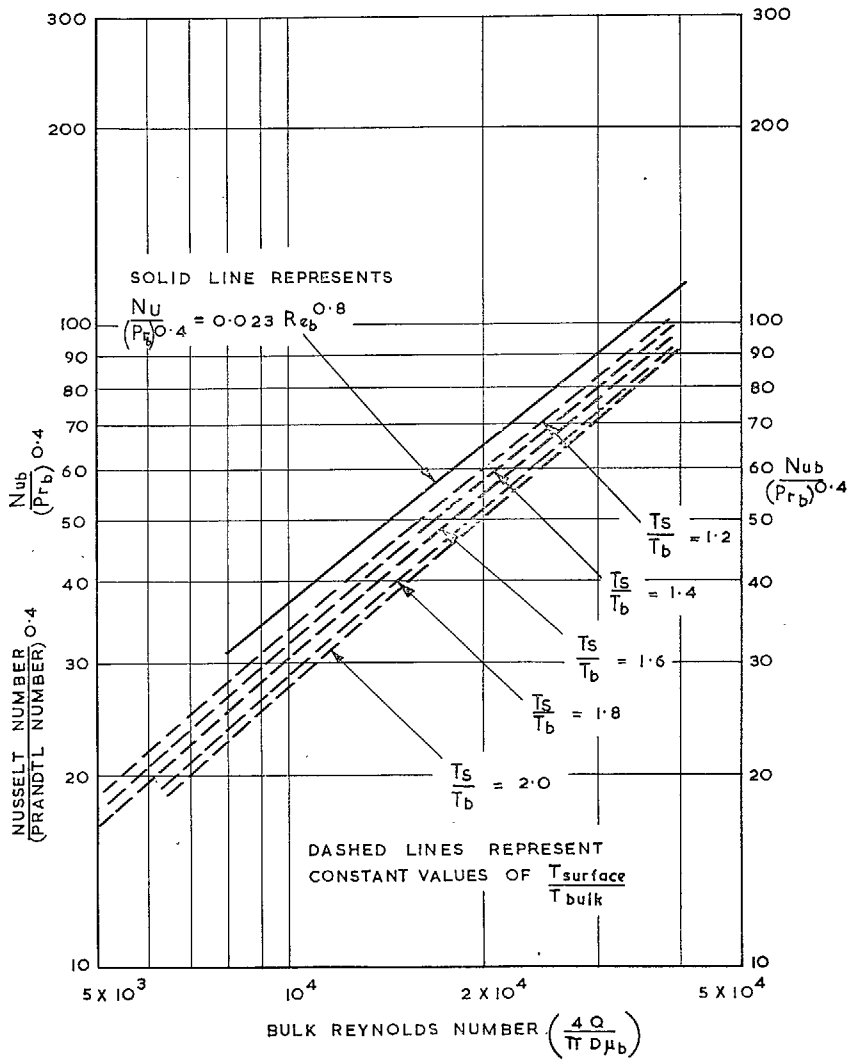

FIG. 11. Summary of carbon dioxide heat transfer results with all gas properties evaluated at T_b.
(300 *deg.* $K < T_b <$ 400 *deg.* K) and (300 *deg.* $K < T_s <$ 800 *deg.* K).

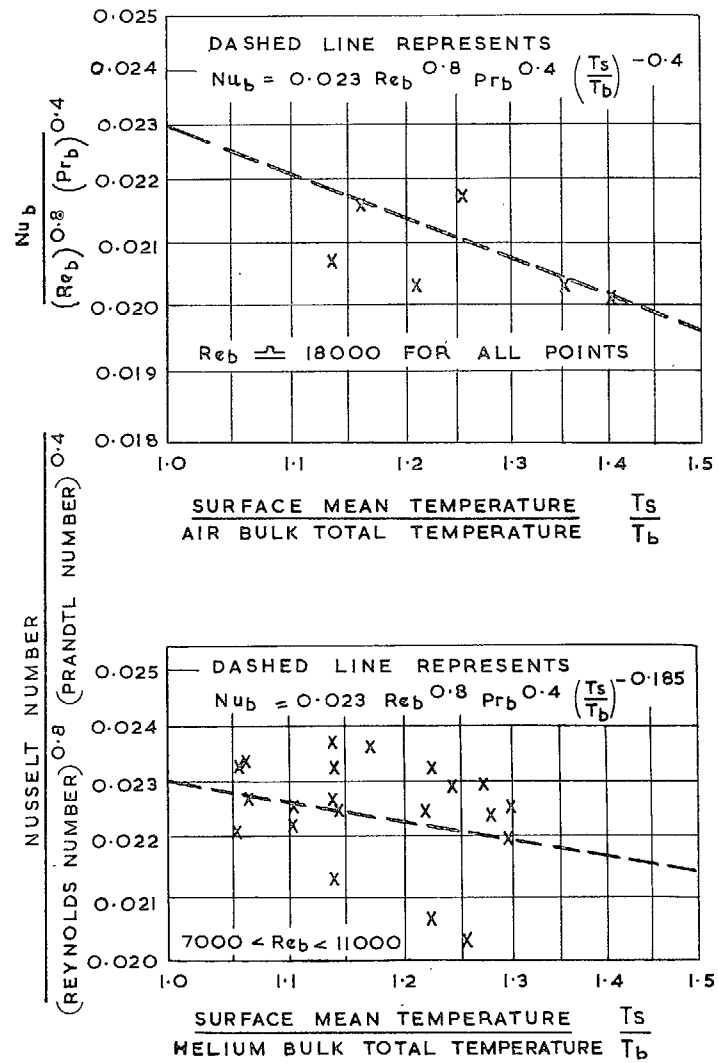

FIG. 12. Experimental heat transfer results for air and helium with all gas properties evaluated at T_b.
(580 *deg.* $K < T_b <$ 670 *deg.* K.)

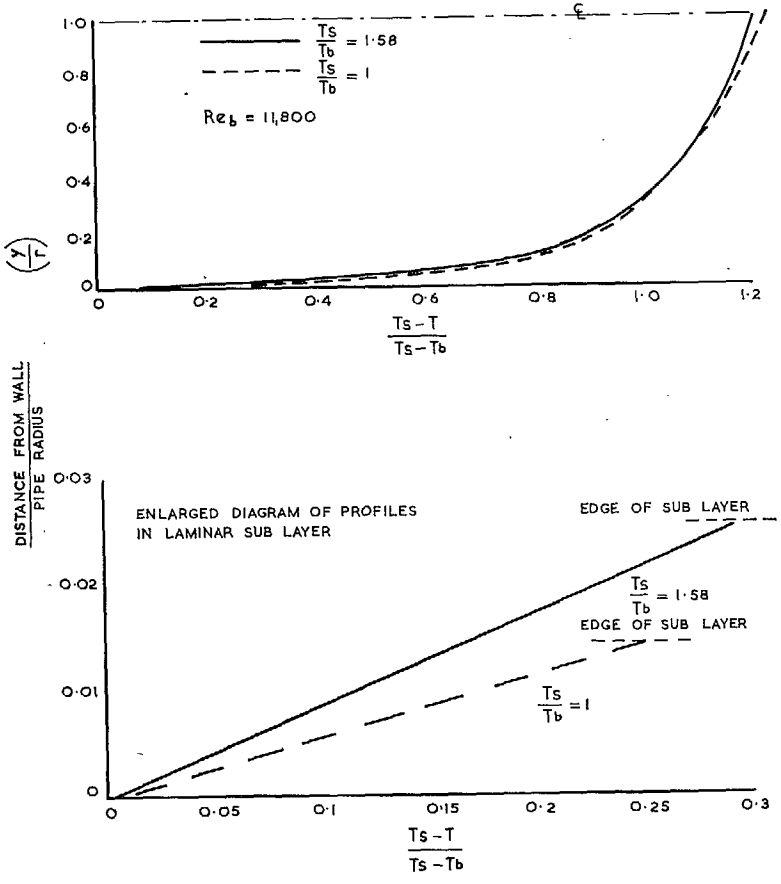

FIG. 13. Temperature profiles (helium).
($T_s/T_b = 1{\cdot}58$ and 1, $Re_b = 11{,}800$.)

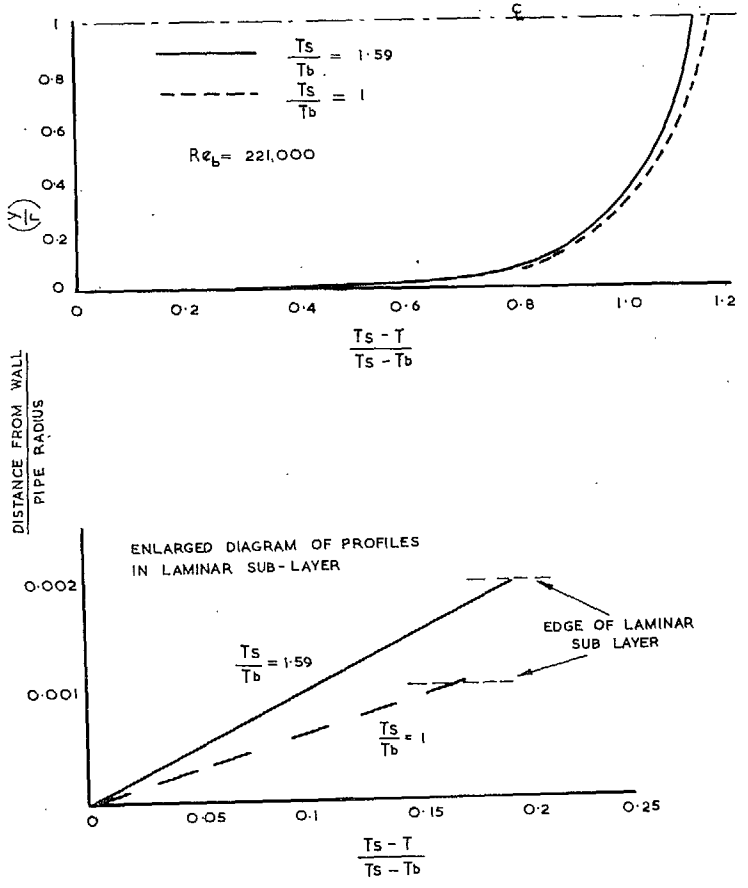

FIG. 14. Temperature profiles (helium).
($T_s/T_b = 1{\cdot}59$ and 1, $Re_b = 221{,}000$.)

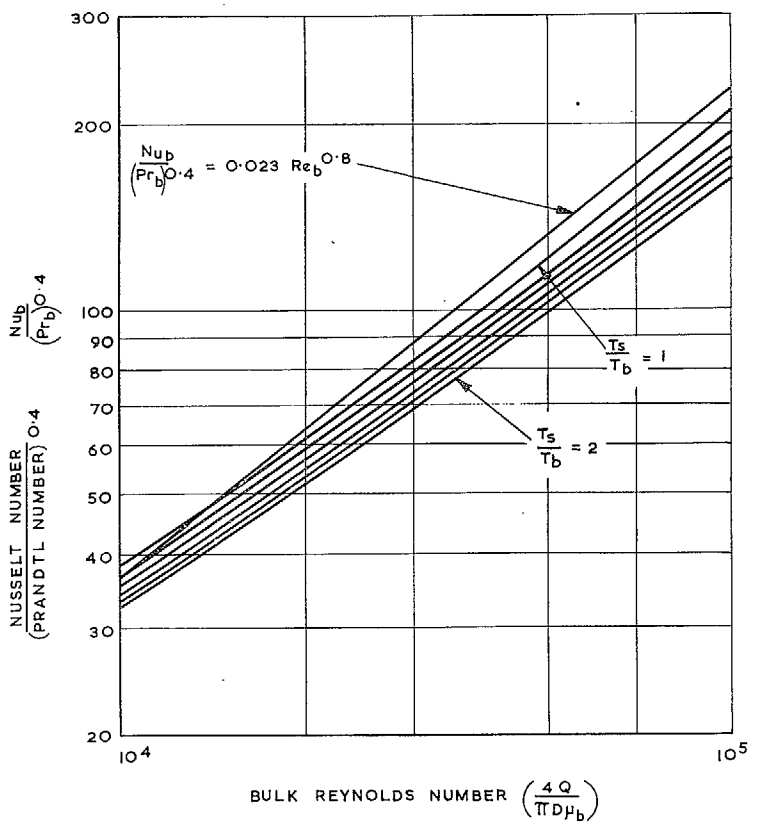

FIG. 15. Theoretical heat transfer data for helium. (Calculated from Reference 6.)

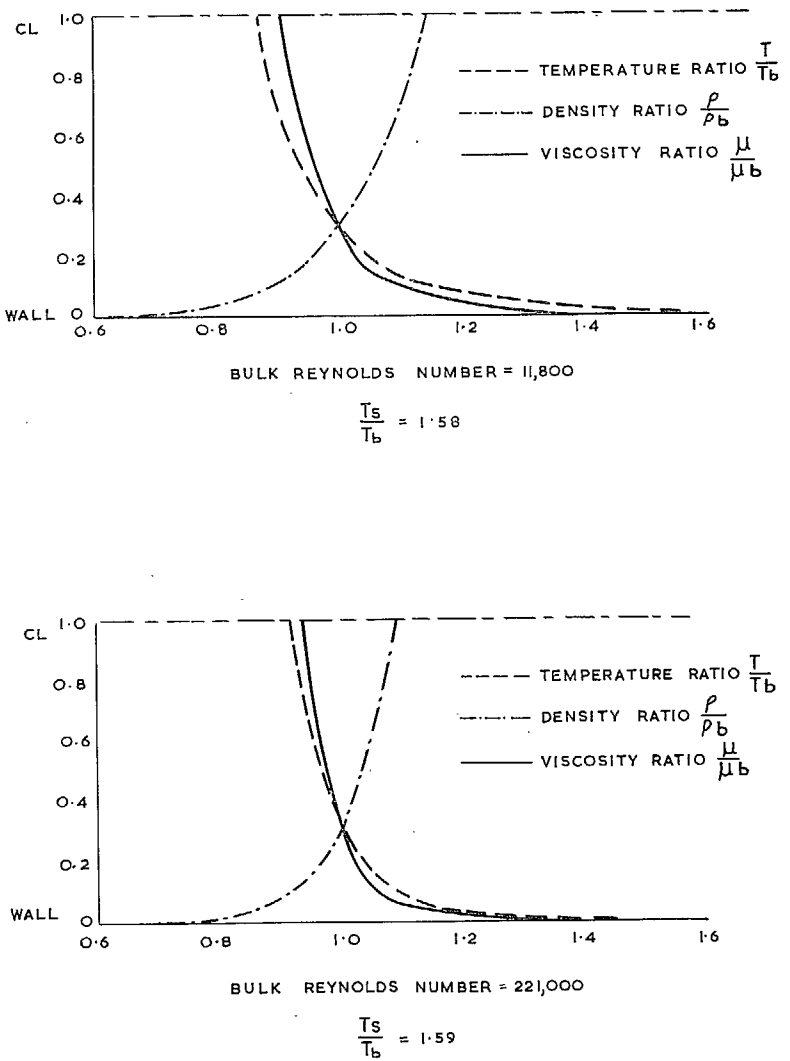

FIG. 16. Helium temperature, density and viscosity profiles for T_s/T_b 1·6, showing effect of Reynolds number.

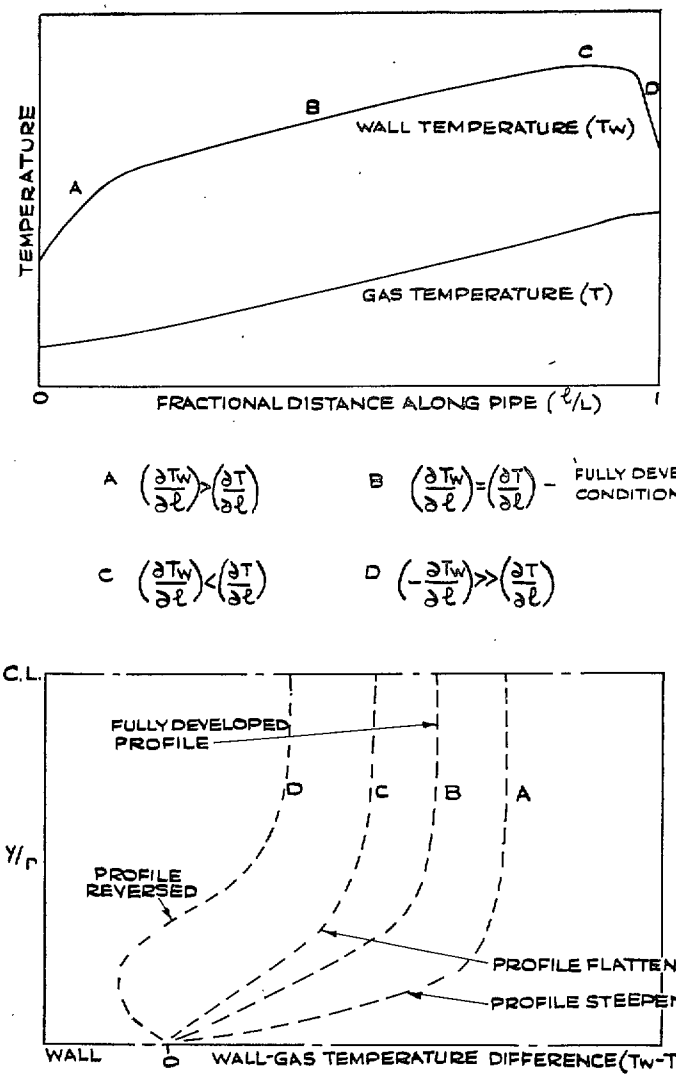

FIG. 17. Diagram showing effects of axial wall temperature gradients on gas radial temperature profiles.

(83191) Wt. 67/1876 K.5 12/61 Hw.

Publications of the Aeronautical Research Council

ANNUAL TECHNICAL REPORTS OF THE AERONAUTICAL RESEARCH COUNCIL (BOUND VOLUMES)

1941 Aero and Hydrodynamics, Aerofoils, Airscrews, Engines, Flutter, Stability and Control, Structures. 63*s.* (post 2*s.* 3*d.*)

1942 Vol. I. Aero and Hydrodynamics, Aerofoils, Airscrews, Engines. 75*s.* (post 2*s.* 3*d.*)
Vol. II. Noise, Parachutes, Stability and Control, Structures, Vibration, Wind Tunnels. 47*s.* 6*d.* (post 1*s.* 9*d.*)

1943 Vol. I. Aerodynamics, Aerofoils, Airscrews. 80*s.* (post 2*s.*)
Vol. II. Engines, Flutter, Materials, Parachutes, Performance, Stability and Control, Structures. 90*s.* (post 2*s.* 3*d.*)

1944 Vol. I. Aero and Hydrodynamics, Aerofoils, Aircraft, Airscrews, Controls. 84*s.* (post 2*s.* 6*d.*)
Vol. II. Flutter and Vibration, Materials, Miscellaneous, Navigation, Parachutes, Performance, Plates and Panels, Stability, Structures, Test Equipment, Wind Tunnels. 84*s.* (post 2*s.* 6*d.*)

1945 Vol. I. Aero and Hydrodynamics, Aerofoils. 130*s.* (post 3*s.*)
Vol. II. Aircraft, Airscrews, Controls. 130*s.* (post 3*s.*)
Vol. III. Flutter and Vibration, Instruments, Miscellaneous, Parachutes, Plates and Panels, Propulsion. 130*s.* (post 2*s.* 9*d.*)
Vol. IV. Stability, Structures, Wind Tunnels, Wind Tunnel Technique. 130*s.* (post 2*s.* 9*d.*)

1946 Vol. I. Accidents, Aerodynamics, Aerofoils and Hydrofoils. 168*s.* (post 3*s.* 3*d.*)
Vol. II. Airscrews, Cabin Cooling, Chemical Hazards, Controls, Flames, Flutter, Helicopters, Instruments and Instrumentation, Interference, Jets, Miscellaneous, Parachutes. 168*s.* (post 2*s.* 9*d.*)
Vol. III. Performance, Propulsion, Seaplanes, Stability, Structures, Wind Tunnels. 168*s.* (post 3*s.*)

1947 Vol. I. Aerodynamics, Aerofoils, Aircraft. 168*s.* (post 3*s.* 3*d.*)
Vol. II. Airscrews and Rotors, Controls, Flutter, Materials, Miscellaneous, Parachutes, Propulsion, Seaplanes, Stability, Structures, Take-off and Landing. 168*s.* (post 3*s.* 3*d.*)

Special Volumes

Vol. I. Aero and Hydrodynamics, Aerofoils, Controls, Flutter, Kites, Parachutes, Performance, Propulsion, Stability. 126*s.* (post 2*s.* 6*d.*)
Vol. II. Aero and Hydrodynamics, Aerofoils, Airscrews, Controls, Flutter, Materials, Miscellaneous, Parachutes, Propulsion, Stability, Structures. 147*s.* (post 2*s.* 6*d.*)
Vol. III. Aero and Hydrodynamics, Aerofoils, Airscrews, Controls, Flutter, Kites, Miscellaneous, Parachutes, Propulsion, Seaplanes, Stability, Structures, Test Equipment. 189*s.* (post 3*s.* 3*d.*)

Reviews of the Aeronautical Research Council

1939–48 3*s.* (post 5*d.*) 1949–54 5*s.* (post 5*d.*)

Index to all Reports and Memoranda published in the Annual Technical Reports

1909–1947 R. & M. 2600 6*s.* (post 2*d.*)

Indexes to the Reports and Memoranda of the Aeronautical Research Council

Between Nos. 2351–2449	R. & M. No. 2450 2*s.* (post 2*d.*)
Between Nos. 2451–2549	R. & M. No. 2550 2*s.* 6*d.* (post 2*d.*)
Between Nos. 2551–2649	R. & M. No. 2650 2*s.* 6*d.* (post 2*d.*)
Between Nos. 2651–2749	R. & M. No. 2750 2*s.* 6*d.* (post 2*d.*)
Between Nos. 2751–2849	R. & M. No. 2850 2*s.* 6*d.* (post 2*d.*)
Between Nos. 2851–2949	R. & M. No. 2950 3*s.* (post 2*d.*)
Between Nos. 2951–3049	R. & M. No. 3050 3*s.* 6*d.* (post 2*d.*)

HER MAJESTY'S STATIONERY OFFICE

from the addresses overleaf

Printed and published by
HER MAJESTY'S STATIONERY OFFICE

To be purchased from
York House, Kingsway, London W.C.2
423 Oxford Street, London W.1
13A Castle Street, Edinburgh 2
109 St. Mary Street, Cardiff
39 King Street, Manchester 2
50 Fairfax Street, Bristol 1
2 Edmund Street, Birmingham 3
80 Chichester Street, Belfast 1
or through any bookseller

Printed in England

S.O. Code No. 23-3246